The Astrophysical Journal, 604:579–595, 2004 April 1
© 2004. The American Astronomical Society. All rights reserved. Printed in U.S.A.

CAN A "STANDARD" INITIAL MASS FUNCTION EXPLAIN THE METAL ENRICHMENT IN CLUSTERS OF GALAXIES?

L. Portinari,[1] A. Moretti,[2,3] C. Chiosi,[2] and J. Sommer-Larsen[1]

Received 2003 August 29; accepted 2003 December 17

ABSTRACT

It is frequently debated in literature whether a "standard" initial mass function (IMF)—meaning an IMF of the kind usually adopted to explain the chemical evolution in the local solar neighborhood—can account for the observed metal enrichment and iron mass-to-light ratio in clusters of galaxies. We address this problem by means of straightforward estimates that should hold independently of the details of chemical evolution models. It is crucial to compute self-consistently the amount of mass and metals locked-up in stars by accounting for the stellar mass-to-light ratio predicted by a given IMF. It then becomes clear that a "standard" solar neighborhood IMF cannot provide enough metals to account for the observed chemical properties in clusters: clusters of galaxies and the local environment must be characterized by different IMFs. Alternatively, if we require the IMF to be universal, in order to explain clusters such an IMF must be much more efficient in metal production than usually estimated for the solar vicinity. In this case, substantial loss of metals is required from the solar neighborhood and from disk galaxies in general. This "nonstandard" scenario of the local chemical evolution would challenge our present understanding of the Milky Way and of disk galaxy formation.

Subject headings: galaxies: abundances — galaxies: clusters: general — galaxies: evolution — intergalactic medium — stars: luminosity function, mass function

1. INTRODUCTION

There seems to be no consensus in the literature as to whether a "standard" initial mass function (IMF)—by which term we indicate an IMF of the kind generally adopted to explain the chemical properties of the solar vicinity, in the standard models with infall and no outflows—can account for the observed level of metal enrichment and iron mass-to-light ratio (Ciotti et al. 1991; Renzini et al. 1993) in clusters of galaxies.

The efficiency of metal enrichment from a stellar population is estimated by computing the global (or net) yield (Tinsley 1980; Pagel 1997):

$$y = \frac{1}{1-R}\int_{M_{\rm TO}(t)}^{M_s} p_Z(M)\Phi(M)\,dM, \qquad (1)$$

where $M_{\rm TO}(t)$ is the turnoff stellar mass of lifetime corresponding to the age t of the population, M_s is the upper mass limit of the IMF, $p_Z(M)$ is the mass fraction of newly synthesized metals ejected by a star of mass M, and $\Phi(M)$ is the IMF. Hence the integral expresses the amount of metals globally produced by a stellar generation up to its present age. R represents the "returned fraction" of gas re-ejected by dying stars, so that $1-R$ is the fraction of mass locked up in living stars and remnants. According to the definition of the net yield,[4] the efficiency of metal enrichment depends not just on the amount of metals produced per mass involved in star formation but on the ratio between this and the mass that remains locked in stars. The locked-up fraction, related to the number of ever-lived low-mass stars in the IMF, is as crucial to the overall enrichment as is the number of the high-mass stars directly responsible for the production of metals. By "ever-lived stars" we mean stars with lifetimes longer than a Hubble time, typically $M < 0.9\ M_\odot$.

As pointed out by Arnaud et al. (1992), it would be surprising if the same "recipe" could account at the same time for the solar vicinity and for galaxy clusters, since the observed yield is definitely very different in the two environments. In the solar vicinity the gas mass is ~20% of the stellar mass and its metallicity is $\sim Z_\odot$, while in clusters of galaxies the intracluster gas mass is estimated to be 5–10 times the stellar mass (Arnaud et al. 1992; Lin et al. 2003) and its typical metallicity is $\sim 0.3\ Z_\odot$. The stellar metallicity, on the other hand, is comparable (roughly solar) in the two environments. This naive estimate outlines the difference between clusters and the solar vicinity:

$$y_{\rm SV} \sim \frac{Z_\odot M_* + Z_\odot(0.2M_*)}{M_*} = 1.2\ Z_\odot, \qquad (2)$$

$$y_{\rm cl} \sim \frac{Z_\odot M_* + 0.3Z_\odot[(5\text{–}10)M_*]}{M_*} = 2.5 - 4\ Z_\odot \qquad (3)$$

(see also Pagel 2002). The difference is possibly larger than this, since the typical metallicity of the stellar populations in clusters may be higher than the local one: galaxies in clusters are in fact dominated in mass by the bright ellipticals with metallicities between solar and supersolar, while in the solar vicinity the metallicity distribution peaks around −0.2 dex. We assess in detail the observed yield in the solar neighborhood versus cluster in the Appendix, distinguishing iron from α-elements. All in all, the observed yield in clusters is 3–4 times larger than in the solar vicinity.

[1] Theoretical Astrophysics Center, Juliane Maries Vej 30, DK-2100 Copenhagen Ø, Denmark; lportina@tac.dk, jslarsen@tac.dk.

[2] Department of Astronomy, University of Padova, Vicolo dell'Osservatorio 2, I-35122 Padua, Italy; moretti@pd.astro.it, chiosi@pd.astro.it.

[3] INAF, Observatory of Padova, Vicolo dell'Osservatorio 5, I-35122 Padua, Italy.

[4] In this paper, the term "yield" will generally indicate the net yield y of a stellar population as defined in eq. (1); we will explicitly speak, instead, of "stellar yields" to indicate the $p_Z(M)$ resulting from nucleosynthesis calculations.

Gaseous inflows and outflows can alter the "apparent" or "effective yield," as deduced from the observed metallicities, with respect to the "true" net yield of the underlying stellar population as defined in equation (1) (Edmunds 1990; Edmunds & Greenhow 1995; Pagel 1997). However, it is hard to imagine gas flows to be so prominent on the scale of clusters as to substantially modify the apparent yield over such large scales and masses. It might be somewhat easier, although still a complex issue, to invoke these effects on the scale of individual galaxies and of the solar vicinity (see our conclusions in § 5.2). The effect of flows is in fact, in most cases, to decrease the apparent yield below the true yield.

As a consequence of the strikingly different observed yield, many authors resorted to "nonstandard" IMFs to explain the level of metal enrichment in clusters, invoking in turn top-heavy IMFs (David et al. 1991a; Matteucci & Gibson 1995; Gibson & Matteucci 1997a, 1997b; Loewenstein & Mushotzky 1996), bimodal IMFs (Arnaud et al. 1992; Elbaz et al. 1995), variable IMFs (Chiosi 2000; Moretti et al. 2003; Finoguenov et al. 2003), or contribution from Population III hypernovas (Loewenstein 2001; Baumgartner et al. 2003).

On the other hand, the arguments brought in favor of an invariant, standard IMF are (1) that the iron mass-to-light ratio (IMLR) observed in clusters is compatible with the predictions from the Salpeter IMF (Renzini et al. 1993; Renzini 1997, 2003) and (2) that the [α/Fe] abundance ratios in the intracluster medium (ICM) are compatible, within uncertainties, with those in the Sun and in local disk stars (Ishimaru & Arimoto 1997; Wyse 1997; Renzini 1997, 2003). However, neither of these two diagnostics is sensitive to the amount of mass (and metals!) locked–up in low-mass stars. Very low mass, ever-lived stars do not contribute metals or luminosity, but they act as an effective *sink* of metals. This effect is crucial for determining the partition of metals between the stars and the ICM:

1. Let us define the typical IMLR expected from a stellar population with a given IMF as

$$\mathrm{IMLR_{SSP}} = \frac{M\mathrm{Fe}}{L_B},$$

where L_B is the luminosity of a single stellar population (SSP) of initial mass 1 $M_\odot$ and MFe is the iron mass produced by the same SSP. Consider, as an example, two Salpeter IMFs differing only in the low-mass limit, say [0.1–100] $M_\odot$ and [0.5–100] $M_\odot$, respectively: these two IMFs have the same typical $\mathrm{IMLR_{SSP}}$, because stars between 0.1 and 0.5 $M_\odot$ contribute neither metals nor substantial luminosity. However, these IMFs imply, *for the same* $\mathrm{IMLR_{SSP}}$ *and observed stellar metallicity*, very different amounts of mass and metals locked up in the stellar component, correspondingly changing the remaining fraction of the produced metals available to enrich the ICM.

2. Similarly, [α/Fe] abundance ratios trace the *relative* proportion of Types II and Ia supernovas (SNe II and SNe Ia), that is to say the relative number of massive stars with respect to intermediate (down to ~solar) mass stars. This is sensitive to the shape and slope of the IMF above ~1 $M_\odot$, but it is insensitive to the amount of mass locked in ever-lived stars of lower mass (as acknowledged in fact by Wyse 1997) or to the *global* amount of metals produced.

The amount of mass locked in low-mass, ever-lived stars is strictly related to the stellar mass-to-light ratio (M/L) predicted by a given IMF (Renzini et al. 1993). In this paper we stress the importance of taking into account self-consistently the stellar M/L, in order to understand whether a standard IMF can in fact explain the observed metal enrichment of clusters of galaxies.

Our approach is very straightforward: for any given IMF, one can compute the corresponding rates of SNe II and SNe Ia and the rate of production of iron $M\mathrm{Fe_{tot}}(t)$ (Figs. 1*a* and 1*b*)—or of any other element. For the same IMF, the corresponding SSP derived from stellar isochrones gives the luminosity evolution $L_B(t)$ (Fig. 1*c*), and the ratio $M\mathrm{Fe_{tot}}(t)/L_B(t)$ gives the typical $\mathrm{IMLR_{SSP}}(t)$ expected from the stellar population as a function of its age (Fig. 1*d*). Of course, $\mathrm{IMLR_{SSP}}$ is not the IMLR observed in the ICM, since part of the metals produced will be "eaten up" by successive stellar populations to build up the observed stellar metallicities in cluster galaxies. Therefore, our second step is to consider the mass in stars and the fraction of metals locked in stars *consistent* with the adopted IMF and with the observed stellar metallicities; only what remains out of the global metal production is in principle available to enrich the ICM and can be compared with the observed ICM metallicity.

We will discuss two cases of IMF: the Salpeter IMF (mostly for comparison and discussion of previous literature; § 2) and the Kroupa IMF (an example of "standard" IMF for the solar neighborhood; § 3). In § 4 we will discuss our results, which clearly indicate that a Salpeter IMF—and even less a standard solar neighborhood IMF—is unable to account for the level of metal enrichment in clusters of galaxies; these results are robust with respect to uncertainties concerning the theoretical stellar yields, the rate of SNe Ia, and the details in the star formation history of cluster galaxies. We also outline the qualitative features of an IMF that should be able to reproduce clusters of galaxies. Finally, in § 5 we conclude that we are left either with a nonuniversal IMF (different between clusters and solar neighborhood) or with a nonstandard scenario for the chemical evolution of the solar neighborhood; we discuss each possibility in turn.

2. PREDICTIONS FROM THE SALPETER IMF

We will first discuss the most "classic" case, the Salpeter (1955) IMF with constant power-law slope and mass limits [0.1–100] $M_\odot$; all the computations in this section, as well as the terms "Salpeter IMF" or "Salpeter SSP" hereafter, refer to the above-mentioned mass limits.

We remark, though, that the Salpeter IMF is *not* a "standard" IMF in the sense explained in the introduction: it is *too efficient* in metal enrichment, i.e., its typical global yield is too high, to match the typical abundances in the solar neighborhood and in disk galaxies in standard chemical evolution models (Tsujimoto et al. 1997; Thomas et al. 1998; Gratton et al. 2000; Portinari et al. 2004). Besides, from observed star counts in the solar neighborhood and arguments related to the stellar M/L in disk galaxies, there is by now a general consensus that the IMF is not a single-slope power law extrapolated down to 0.1 $M_\odot$, but it "bends over" below ~1 $M_\odot$, implying a smaller percentage of low-mass stars (Kroupa 2001, 2002; Chabrier 2003; Portinari et al. 2004 and references therein).

Nevertheless, the "classic" Salpeter IMF is still very widely adopted in literature for chemical and spectrophotometric

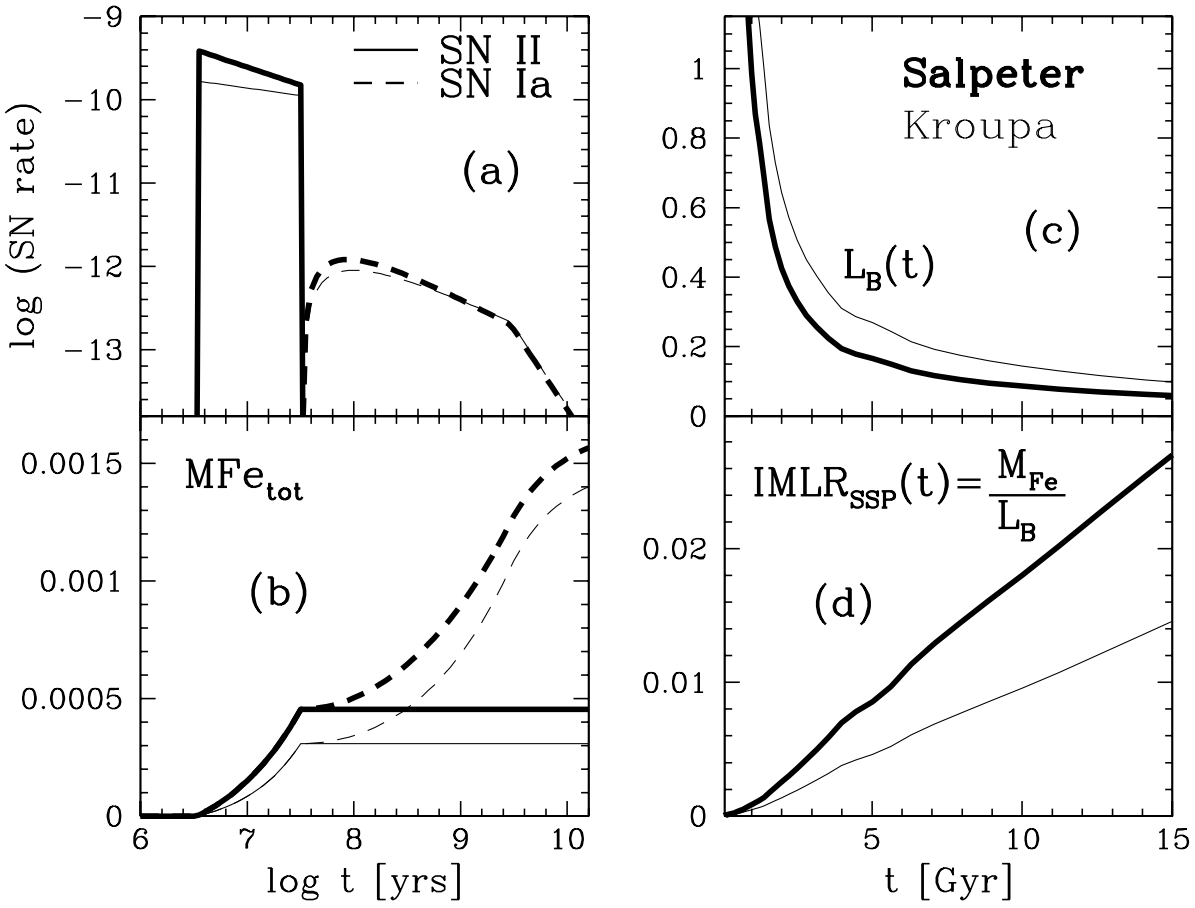

FIG. 1.—(*a*) Evolution of the rate of SNe II and SNe Ia, in number per year, for a Salpeter and a Kroupa SSP of 1 $M_\odot$ (*thick and thin lines, respectively*). (*b*) Corresponding cumulative iron production from SNe II and SNe Ia, in $M_\odot$. (*c*) *B*-band luminosity evolution of a Salpeter and a Kroupa SSP of 1 $M_\odot$, in $L_{B,\odot}$. (*d*) Evolution of the characteristic $\mathrm{IMLR_{SSP}}$ of a Salpeter and a Kroupa SSP.

models, and it has often been adopted to model clusters of galaxies, so it is mandatory to consider it for the sake of comparison and to comment on literature results.

2.1. *Metal Production*

Let us compute the amount of newly synthesized metals expected to be released by a Salpeter SSP of initial mass 1 $M_\odot$. Adopting the chemical yields by Portinari et al. (1998), a Salpeter SSP produces

$$M\mathrm{O_{II}} = 0.01\ M_\odot,$$

$$M\mathrm{Fe_{II}} = 4.8 \times 10^{-4}\ M_\odot$$

of new ^{16}O and ^{56}Fe from SNe II. This estimate takes into account that the original SN models by Woosley & Weaver (1995), which were ultimately the base for the Portinari et al. yields, are too efficient in iron production. Here we decreased the iron yield of SNe II by a factor of 1.5, so that the typical [O/Fe] ratio of SN II ejecta is [O/Fe]$\sim+0.5$ as indicated by abundances in halo stars.[5] This amount of iron production is in close agreement with the following rule-of-thumb estimate: with a Salpeter IMF, a 1 $M_\odot$ SSP results in 7.4×10^{-3} SNe II ($M > 8\ M_\odot$), and each of these produces on average 0.07 $M_\odot$ of ^{56}Fe (like SN 1987a). We neglect here the metallicity dependence of stellar yields, which for oxygen and iron becomes relevant only for $Z > Z_\odot$.

The release of new oxygen and iron by SNe II can be considered instantaneous for the purpose of this paper. The iron from SNe Ia is released instead over longer timescales (Figs. 1*a* and 1*b*). We adopt the SN Ia rate formalism by Greggio & Renzini (1983), with the classic mass limits [3–16] $M_\odot$ and frequency coefficient $A = 0.07$ for the binary systems progenitors of SNe Ia; this calibration is suited to reproduce the typical SN II/SN Ia ratio in Milky Way–type galaxies and the evolution of the abundance ratios in the solar neighborhood (Chiappini et al. 1997; Portinari et al. 1998).

In Figure 2 we plot the SN Ia rate for our SSPs in SN units (SNu; number of SNe per 100 yr per $10^{10} L_{B,\odot}$) and compare it with observational estimates. The rate in SNu is obtained as the ratio of the SN Ia rate of the SSP (Fig. 1*a*) versus the corresponding luminosity evolution $L_B(t)$ (Fig. 1*c*). Just like the $\mathrm{IMLR_{SSP}}$ or the relative number of SNe II versus SNe Ia, the SN rate in SNu is independent of the amount of mass locked in very low mass stars: it is sensitive to the shape of the IMF only above about 1 $M_\odot$, whence both SN and luminosity originate. We compare our SSP predictions with the local SN rate in elliptical galaxies (Cappellaro 2001), where the stellar population, with an early and short star formation history, more closely resembles an SSP. The local SN rate in ellipticals

[5] We adopt as solar abundances $[\mathrm{O/H}]_\odot = 8.87$, $[\mathrm{Si/H}]_\odot = 7.55$ and $[\mathrm{Fe/H}]_\odot = 7.5$ (Grevesse et al. 1996). Notice that the recent photospheric abundance of iron is in excellent agreement with the meteoritic value (Grevesse & Sauval 1999). These abundances correspond to mass fractions of $X_\mathrm{O} = 8.3 \times 10^{-3}$, $X_\mathrm{Si} = 6.9 \times 10^{-4}$, and $X_\mathrm{Fe} = 1.2 \times 10^{-3}$, respectively, i.e., to an oxygen mass 7 times larger than the iron mass in the Sun.

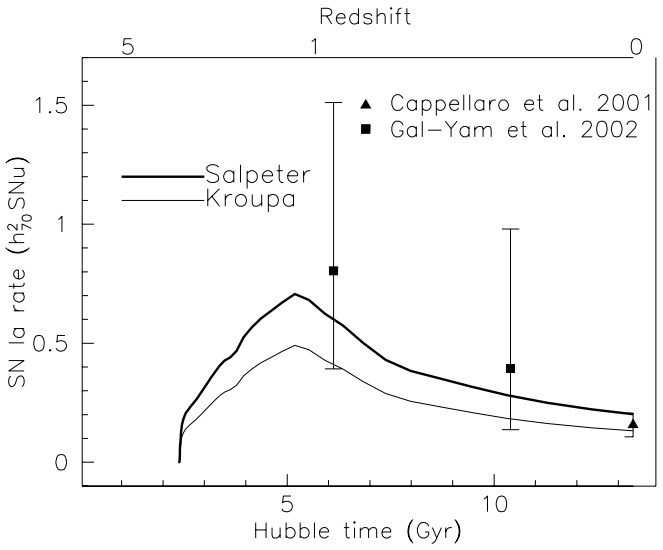

FIG. 2.—Evolution of the SN Ia rate (in SNu) with respect to Hubble time, for a Salpeter and a Kroupa SSP (*thick and thin lines, respectively*) of 11 Gyr of age. Data from Cappellaro (2001) and Gal-Yam et al. (2002).

is very well matched by our models, which is remarkable since our SN Ia prescription is suited and calibrated for the solar neighborhood.

At redshift $z > 0$, we compare our predictions with the results from an *Hubble Space Telescope* high-redshift search for SNe Ia in clusters (Gal-Yam et al. 2002; Maoz & Gal-Yam 2004)—thus mostly sampling elliptical galaxies. The agreement is also good at higher redshift, considering that we are adopting a "standard solar neighborhood" SN Ia prescription. In Figure 2 we assumed an age of 11 Gyr for the SSP; but the agreement with the data is acceptable for SSP ages between 10 and 12 Gyr.

We compute and list in Table 1 the cumulative number $N_{\rm Ia}$ of SNe Ia in a Salpeter SSP as a function of time and also the related iron production $M{\rm Fe}_{\rm Ia}$. We assume that each SN Ia produces 0.7 $M_\odot$ of iron. By the end of the evolution, the number of SNe Ia is about $\frac{1}{4}$ of that of SNe II and the iron contribution is $\frac{1}{3}$ from SNe II and $\frac{2}{3}$ from SNe Ia (see also Fig. 1*b*). These values are compatible with the solar proportions, but we stress that these represent *relative* proportions while the *global* metal production depends on the mass limits of the IMF, i.e., its normalization.

The oxygen production from SNe Ia is minor: each SN Ia produces 0.143 $M_\odot$ of oxygen (Iwamoto et al. 1999), so globally, for a Salpeter SSP, SNe Ia altogether contribute

$$M{\rm O}_{\rm Ia} = 2 \times 10^{-4}\ M_\odot,$$

absolutely negligible with respect to the SN II production. In column (8) of Table 1 we list the typical [O/Fe] ratio of the global metal production (SNe II+SNe Ia) of the SSP as a function of time. For $t > 5$ Gyr the [O/Fe] ratio is roughly solar (see also Fig. 6*b*, *solid line*).

2.2. *Luminosity, Stellar Mass, and IMLR*

We now derive the typical ${\rm IMLR}_{\rm SSP}$ by combining the global iron production $M{\rm Fe}_{\rm tot}(t)$ in Table 1 and Figure 1*b*, with the luminosity evolution of a Salpeter SSP. In Figure 1*c* we show the luminosity evolution for a Salpeter IMF computed from the isochrones by Girardi et al. (2002) with solar metallicity and $\mathcal{M}_{B\odot} = 5.489$; in Figure 1*d* we show the corresponding evolution of the characteristic ${\rm IMLR}_{\rm SSP} = M{\rm Fe}_{\rm tot}/L_B$. The values of L_B and ${\rm IMLR}_{\rm SSP}$ for some representative ages are listed in Table 2.

The observed IMLR in the ICM is ${\rm IMLR}_{\rm ICM} \sim 0.01$–$0.015\ M_\odot/L_\odot$ (Finoguenov et al. 2000, 2001; De Grandi et al. 2003).[6] From Table 2 and Figure 1*d*, we can anticipate that the ${\rm IMLR}_{\rm SSP}$ of a Salpeter SSP *can* be compatible with the ${\rm IMLR}_{\rm ICM}$ observed in the ICM provided that we are dealing

[6] We note that the iron abundances measured in the ICM are often expressed in terms of the old photospheric value for the solar iron abundance by Anders & Grevesse (1989). More recent photospheric values agree instead with the meteoritic value, which is lower by ~0.17 dex, i.e., a factor of 1.5 in mass/number abundance (see also footnote 2) . This has induced a great deal of confusion on the interpretation of the abundance ratios in the ICM (Ishimaru & Arimoto 1997; Wyse 1997). While the latest X-ray studies have started to refer consistently to the updated solar iron abundance (Baumgartner et al. 2003; De Grandi et al. 2003), we notice that fortunately the reference solar value adopted in previous years bears no effects on the estimated iron mass or IMLR in the ICM. In fact, in the spectral fits used to infer elemental abundances from X-ray lines, it is the *absolute abundance* by number of the coolants—iron ions in this case—present in the chemical mixture, that ultimately determines the line strength to be compared with the observed one. Whether this absolute abundance is expressed as a fraction of the old or of the updated solar abundance is a secondary issue from the point of view of the *global* iron mass $M{\rm Fe}_{\rm ICM}$. Henceforth, although attention must be paid to the adopted solar values when comparing, e.g., ICM data to Galactic data, fortunately the estimates of global $M{\rm Fe}_{\rm ICM}$ and ${\rm IMLR}_{\rm ICM}$ are robust absolute values and do not scale with different assumptions for the solar abundance (see also Baumgartner et al. 2003).

TABLE 1
EVOLUTION OF THE METAL PRODUCTION FROM A SALPETER SSP

t (Gyr) (1)	$M_{\rm TO}(t)$ (2)	$N_{\rm Ia}$ (3)	$N_{\rm Ia}/N_{\rm II}$ (4)	$M{\rm Fe}_{\rm Ia}$ (5)	$M{\rm Fe}_{\rm al}/M{\rm Fe}_{\rm II}$ (6)	$M{\rm Fe}_{\rm tot}$ (7)	[O/Fe] (8)	$M{\rm Si}_{\rm Ia}$ (9)	$M{\rm Si}_{\rm tot}$ (10)	[Si/Fe] (11)
1.....	2.2	5.5e-4	0.09	3.9e-4	0.8	8.7e-4	+0.22	8.5e-5	8.8e-4	+0.25
2.....	1.6	1.0e-3	0.16	7.0e-4	1.5	1.2e-3	+0.09	1.5e-4	9.5e-4	+0.14
5.....	1.2	1.4e-3	0.22	9.9e-4	2.0	1.5e-3	−0.01	2.2e-4	1.0e-3	+0.06
10.....	1.0	1.55e-3	0.24	1.1e-3	2.3	1.6e-3	−0.04	2.4e-4	1.0e-3	+0.06
15.....	0.9	1.6e-3	0.25	1.1e-3	2.3	1.6e-3	−0.04	2.5e-4	1.0e-3	+0.06

NOTES.—Col. (1): age of the SSP in gigayears; col. (2): corresponding indicative turnoff mass; col. (3): cumulative number of SNe Ia exploded up to age t; col. (4): relative number of SNe Ia vs. SNe II exploded up to age t; col. (5): cumulative iron mass produced by SNe Ia; col. (6): ratio of iron masses produced by SNe Ia and SNe II; col. (7): total iron mass produced up to age t by SNe II+SNe Ia; col. (8): [O/Fe] ratio of the cumulative metal production of the SSP; col. (9): cumulative silicon mass produced by SNe Ia; col. (10): total silicon mass produced up to age t by SNe II+SNe Ia; col. (11):) [Si/Fe] ratio of the cumulative metal production of the SSP.

TABLE 2
EVOLUTION OF LUMINOSITY, M/L, AND IMLR FOR A SALPETER SSP

t (Gyr) (1)	$\mathcal{M}_B$ (2)	L_B ($L_\odot$) (3)	(M_*) (4)	M_*/L_B (5)	$\mathrm{IMLR_{SSP}}$ (6)	$\mathrm{SiMLR_{SSP}}$ (7)
1.....	5.506	0.984	0.78	0.80	8.8e-4	8.9e-4
2.....	6.416	0.426	0.75	1.74	2.8e-3	2.2e-3
5.....	7.435	0.167	0.72	4.31	9.0e-3	6.0e-3
10.....	8.145	0.087	0.71	8.16	1.8e-2	1.1e-2
15.....	8.554	0.059	0.70	12.5	2.7e-2	1.7e-2

NOTES.—Col. (1): age of the SSP in gigayears; col. (2): B-band magnitude of the SSP; col. (3): B-band luminosity of the SSP ($\mathcal{M}_{B\odot} = 5.489$); col. (4): mass fraction of the initial 1 $M_\odot$ SSP remaining in stars and remnants; col. (5): M/L of the stellar (plus remnants) component of the SSP; col. (6): global IMLR of the SSP, computed from $M\mathrm{Fe_{tot}}(t)$ in Table 1; col. (7): global SiMLR of the SSP, computed from $M\mathrm{Si_{tot}}(t)$ in Table 1.

with old stellar populations ($t \geq 10$ Gyr) and provided that a large part of the iron gets dispersed into the ICM.

Notice from Figure 1*b* that the bulk of the iron production (70%–80%) from the SSP takes place in fact within the first 2–3 Gyr. An early iron production from SNe Ia is not only in agreement with the empirical estimates of the SN Ia rate in clusters up to redshift $z \sim 1$ (Fig. 2) but also, if SNe Ia contribute a significant fraction of the iron in the ICM, with the fact that the observed ICM iron abundance is invariant in clusters up to $z \sim 1.2$ (Tozzi et al. 2003). The evolution of the $\mathrm{IMLR_{SSP}}$ at late times is then dominated by the fading luminosity rather than by late iron production (Figs. 1*c* and 1*d*). Therefore, the age of the stellar population is as crucial to the $\mathrm{IMLR_{SSP}}$ as the amount of iron produced; the presence of a somewhat younger stellar component in the cluster, for instance due to spiral galaxies or late star formation episodes, can significantly reduce the IMLR due to the increased luminosity (cf. $\mathrm{IMLR_{SSP}} < 0.01$ at $t \leq 5$ Gyr.)

To ascertain whether the Salpeter IMF can enrich the ICM to the observed levels, it is now crucial to estimate what fraction of the produced metals is effectively shed into the ICM versus the fraction stored in the stellar component.

2.3. *The Metal Partition between Stars and ICM*

We estimate the amount of metals locked in the stellar component—including living stars and remnants—simply as

$$M\mathrm{Fe}_*(t) = X_{\mathrm{Fe},*} M_*(t), \tag{4}$$

where $X_{\mathrm{Fe},*}$ is the observed metallicity in the stars and $M_*(t)$ is the mass in stars predicted *consistently* from the SSP evolution (Table 2 and Fig. 3). As a consequence, the remaining iron mass available to be dispersed in the ICM is

$$M\mathrm{Fe_{ICM}}(t) = M\mathrm{Fe_{tot}}(t) - M\mathrm{Fe}_*(t), \tag{5}$$

where $M\mathrm{Fe_{tot}}(t)$ is the iron mass globally produced by the SSP, from Figure 1*b* and Table 1. Analogous calculations apply for the partition of other chemical elements.

In equation (5) it may at first look awkward to consider the metals $M\mathrm{Fe}_*$ locked in the stars of an SSP as a fraction of the metals $M\mathrm{Fe_{tot}}$ produced by the same SSP: an SSP is a burst of star formation formed out of gas with some preexisting metallicity, and only later does it release newly synthesized metals; an SSP obviously cannot enrich itself. In real galaxies, the stellar population is not an SSP but the result of a complex star formation history extended in time, even if fast and intensive, as in elliptical galaxies. Subsequent populations lock up part of the metals produced by the previous ones in a way that depends nontrivially on the detailed star formation and inflow and outflow history (Tantalo & Chiosi 2002). Nevertheless, SSP-based computations such as in Tables 1 and 2 give a straightforward estimate of the global amount of metals produced by the stellar populations in the galaxies, and *somehow* a fraction of those metals has been recycled and locked in the stars to reach the observed stellar metallicities. For the purpose of the simple estimates in this paper, the complex star formation and enrichment history of ellipticals can be schematically treated as a "self-enriched SSP."

In Figure 3 we show the evolution of the fraction $M_* = 1 - R$ of the initial mass of the SSP that is locked up in living stars and remnants (see eq. [1]); M_* decreases in time because of gas re-ejection by dying stars over long timescales. In Table 2 we list M_* and the corresponding stellar M/L for some representative ages. The locked-up fraction M_* is derived from the remnant masses by Portinari et al. (1998) for massive stars and by Marigo (2001) for low- and intermediate-mass stars; hence the computation is self-consistent with the luminosity evolution from the isochrones by Girardi et al. (2002): everything is based on the same set of stellar models from the Padua group.

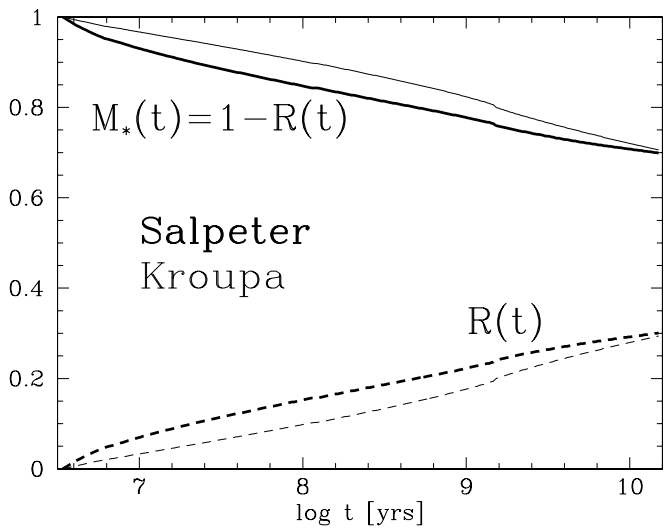

FIG. 3.—Evolution of the returned fraction R and of the complementary locked-up fraction M_* for a Salpeter and a Kroupa SSP (*thick and thin lines, respectively*). Fractions are with respect to the initial mass of the SSP.

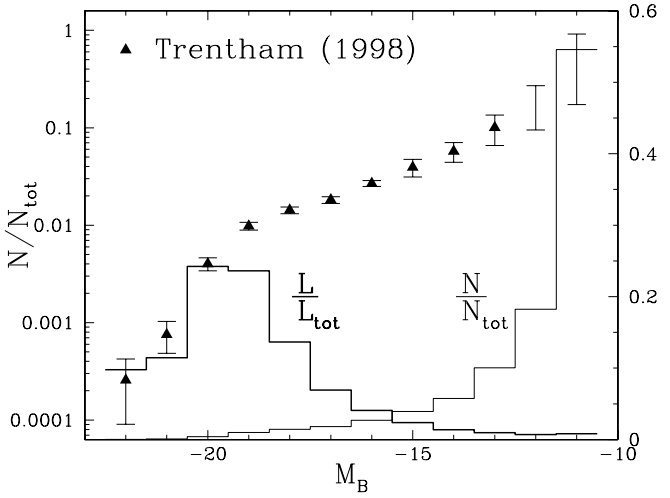

FIG. 4.—Observed cluster luminosity function by Trentham (1998; *triangles and left vertical axis*) and corresponding contribution of the different luminosity bins to the number of galaxies and to the global luminosity (*right axis, in linear scale*). Dwarf galaxies largely dominate in number, but the bulk of the luminosity (and therefore stellar mass) is in massive galaxies with $L \sim L_*$.

We need now an estimate of the typical metallicities of the stellar component in equation (4). Although dwarf galaxies largely dominate in number, the light, stellar mass, and metal production in clusters are dominated by the massive ellipticals (Fig. 4; Thomas 1999; Moretti et al. 2003). These objects have a typical metallicity that is +0.2 dex in the central regions and about solar at the effective radius, with an overall uniform $[\alpha/\mathrm{Fe}] = +0.2$ (Arimoto et al. 1997; Jørgensen 1999; Trager et al. 2000a, 2000b; Mehlert et al. 2003).

In this paper we shall consequently consider two cases for the stellar metallicity, both with relative abundances $[\alpha/\mathrm{Fe}] = +0.2$: case A—global metallicity, dominated by oxygen and α-elements, +0.2 dex and consequently solar iron abundance; and case B—global metallicity and α-element abundances with solar values, and consequently depressed (below solar) iron abundance. Case A seems more representative of the bulk of the stellar mass, which resides in the central regions; case B minimizes the metals locked in the stars, within the range allowed by observations.

In this section we consider case A, corresponding to a solar iron abundance in the stars $X_{\mathrm{Fe},*} = X_{\mathrm{Fe}\odot} = 1.2 \times 10^{-3}$ (see footnote 2 above). In Table 3 we list as a function of age the resulting $M\mathrm{Fe}_*$ and $M\mathrm{Fe}_{\mathrm{ICM}}$ derived from equations (4) and (5) as a function of age. From the typical luminosity $L_B(t)$ of the SSP (Table 2 and Fig. 1*c*), we compute the corresponding IMLR for the stellar and ICM components, respectively. The evolution of the global $\mathrm{IMLR}_{\mathrm{SSP}}$ of a Salpeter SSP, as well as of the separate components $\mathrm{IMLR}_{\mathrm{ICM}}$ and IMLR_*, is plotted in Figure 5*a* (*thick lines*).

In standard galactic wind (GW) models for elliptical galaxies, the wind occurs typically over timescales $\lesssim$1 Gyr, and after the GW no further star formation or metal ejection from the galaxies occurs. From Table 3, if only the gas and metals produced within the first gigayear are ejected from the galaxy into the ICM, very little iron (virtually none) is available to pollute the ICM once the iron in the stars is accounted for. For instance, the models of elliptical galaxies with Salpeter IMF in Chiosi (2000) and Moretti et al. (2003) are characterized by an early GW and eject a negligible amount of iron in the ICM, so that the predicted $\mathrm{IMLR}_{\mathrm{ICM}}$ is an order of magnitude lower than observed. Table 3 shows that, within the framework of the standard GW scenario, the amount of iron that remains locked in the stellar component of a galaxy is not an effect of modeling details, but it is consistently determined by the IMF and the corresponding M/L. Models with the Salpeter IMF and an early GW cannot release substantial amounts of iron to the ICM—if the observed solar stellar abundances are to be reproduced at the same time.

If, on the other hand, all the iron ever produced by the SSP over a Hubble time and not locked in stars is available to be dispersed into the ICM, then it is possible for old SSPs ($t >$ 10 Gyr) to reach the observed levels of $\mathrm{IMLR}_{\mathrm{ICM}}$ (Table 3 and Fig. 7c, *solid line*). This result corresponds to the original conclusion by Matteucci & Vettolani (1988) that, if *all* the iron produced by SNe Ia over long timescales escapes the galaxies, the observed iron mass and IMLR in the ICM can be reproduced. Matteucci & Vettolani (1988) predicted that the late SN Ia ejecta are expelled into the ICM because in the early galactic models the dominant dark matter contribution to the gravitational potential well was not included. When the latter is accounted for, the consensus is that SN Ia products cannot escape the galaxy (David et al. 1991b; Matteucci & Gibson 1995), although recently Pipino et al. (2002) could recover the original result of Matteucci & Vettolani (1988) by allowing for extreme efficiency in the energy feedback of SNe Ia. Alternatively, the late SN Ia ejecta could escape the galaxy via active galactic nucleus feedback or ram-pressure stripping

TABLE 3
PARTITION OF METALS BETWEEN STARS AND ICM WITH THE SALPETER IMF (CASE A)

t (Gyr) (1)	$M\mathrm{Fe}_*$ (2)	$M\mathrm{Fe}_{\mathrm{ICM}}$ (3)	IMLR_* (4)	$\mathrm{IMLR}_{\mathrm{ICM}}$ (5)	$M\mathrm{O}_*$ (6)	$M\mathrm{O}_{\mathrm{ICM}}$ (7)	$[\mathrm{O/Fe}]_{\mathrm{ICM}}$ (8)	$M\mathrm{Si}_*$ (9)	$M\mathrm{Si}_{\mathrm{ICM}}$ (10)	$\mathrm{SiMLR}_{\mathrm{ICM}}$ (11)
1.....	9.4e-4	...	9.6e-4	...	1.0e-2	...	...	8.6e-4	2.8e-5	2.8e-5
2.....	9.0e-4	3.0e-4	2.1e-3	7.0e-4	1.0e-2	...	...	8.2e-4	1.3e-4	3.1e-4
5.....	8.6e-4	6.4e-4	5.0e-3	3.8e-3	9.6e-3	4e-4	−1.05	7.8e-4	2.3e-4	1.4e-3
10.....	8.5e-4	7.5e-4	9.8e-3	8.6e-3	9.5e-3	5e-4	−1.02	7.7e-4	2.6e-4	3.0e-3
15.....	8.4e-4	7.6e-4	1.5e-2	1.4e-2	9.4e-3	6e-4	−0.95	7.7e-4	2.8e-4	4.7e-3

NOTES.—Col. (1): age of the SSP in gigayears; col. (2): iron mass locked in stars and remnants, assuming solar iron abundances for the current stellar mass $M_*(t)$ in Table 2; col. (3): remaining iron mass available to enrich the ICM; col. (4): IMLR of the stellar component, computed from the luminosity $L_B(t)$ in Table 2; col. (5): IMLR of the ICM, provided all the remaining iron can escape the galaxy; col. (6): oxygen mass locked in stars and remnants, assuming $[\mathrm{O/Fe}] = +0.2$ (see text); col. (7): remaining oxygen mass available to enrich the ICM; col. (8): [O/Fe] ratio in the ICM; col. (9): silicon mass locked in stars and remnants, assuming $[\mathrm{Si/Fe}] = +0.2$; col. (10): remaining silicon mass available to enrich the ICM; col. (11): SiMLR of the ICM, provided all the remaining silicon can escape the galaxy.

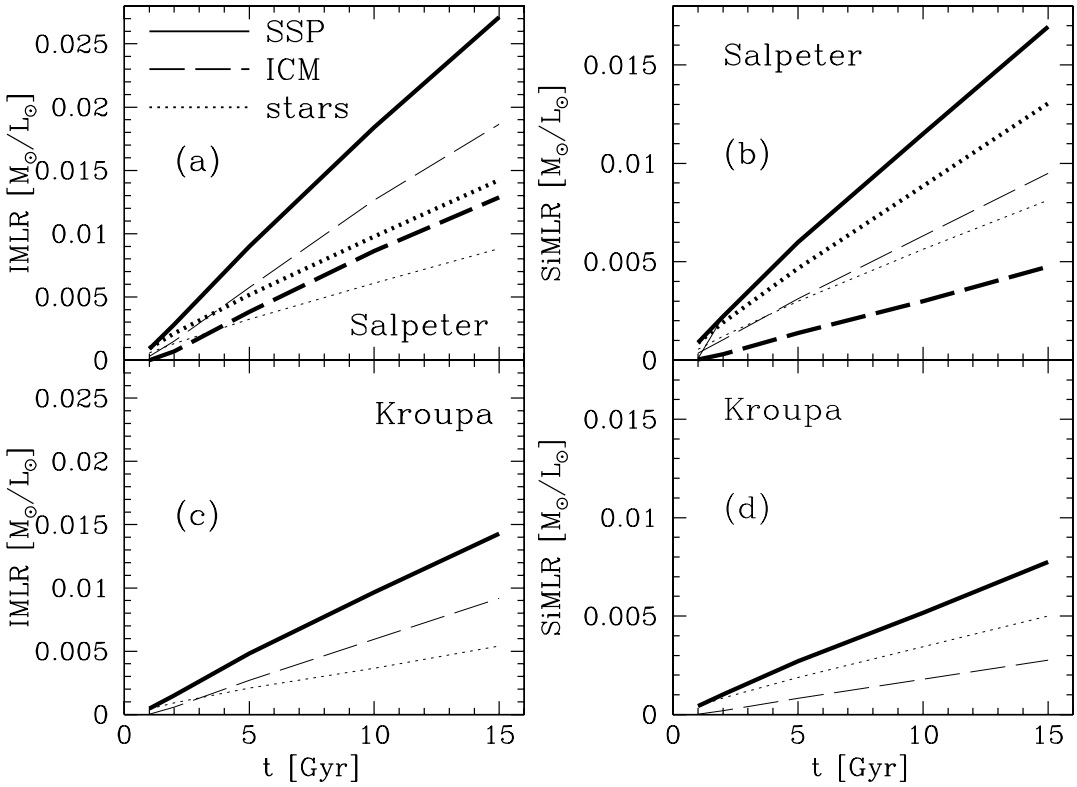

FIG. 5.—Evolution of the IMLR and of the SiMLR for the global SSP ejecta (*solid lines*), for the ICM (*dashed lines*), and for the stellar component (*dotted lines*). Most of the evolution at advanced ages is due to the fading luminosity of the SSP. The partition of metals between stars and ICM is computed self-consistently from the M/L of the SSP, assuming either solar iron abundance (case A; *thick lines*) or solar α-elements abundance in the stars (case B, a "minimal" assumption; *thin lines*). For the Kroupa IMF only case B is considered (*c*, *d*).

(Renzini et al. 1993; see also Ciotti et al. 1991 for the possibility of late outflows from elliptical galaxies).

2.3.1. *The Role of the Stellar M/L*

Notice that for the typical M/L of an old Salpeter SSP and solar iron abundances in the stars (case A), an "equipartition" of iron between stars and ICM is predicted (Renzini et al. 1993)—a behavior not mimicked, however, by α-elements (see § 2.3.2 and Fig. 6 below).

It is the M/L that determines, in the end, the amount of metals locked in the stars and consequently the partition of metals between galaxies and the ICM. In fact, while stellar metallicities can be directly measured from colors and integrated spectral indices, the stellar mass can be estimated only indirectly from the observed luminosity and an assumed M/L. If we are dealing with an old stellar population and a Salpeter IMF, the expected M/L (Table 2) is much larger than that estimated by White et al. (1993) or by Balogh et al. (2001) and often adopted to infer the partition in mass and metals between ICM and galaxies (Renzini 1997, 2003). This is of minor relevance for the problem of the baryonic mass in clusters discussed by White et al. (1993). From dynamical estimates, they adopt $M_*/L_B = 6.4\,h$ and derive $M_*/M_{\rm ICM} \sim 0.1$ (for $h = 0.7$); even with the M/L expected from an old Salpeter IMF, a factor of $\sim$2 higher, the baryonic mass remains largely dominated by the hot ICM mass and the estimated baryon fraction in clusters is very little affected. However, the detailed assumption on the M/L bears much consequence on the estimated "cold fraction" $M_*/M_{\rm ICM}$ (a fundamental constraint on scenarios of cluster formation) (Tornatore et al. 2003; Moretti et al. 2003 and references therein), as well as on the estimated mass of metals locked in stars and on the inferred effective yield in clusters (see the Appendix).

With the low stellar M/L from White et al. (1993), the metal partition is far more skewed toward the ICM, which would contain 2–3 times more iron than galaxies (Renzini 1997, 2003). However, if we assume such low values of M/L, we must conclude correspondingly that the IMF in clusters cannot be the Salpeter IMF but is "bottom-light," meaning with a lower mass fraction locked-up in ever-lived low-mass stars and remnants, and correspondingly with a higher net yield (see eq. [1]). It is thus decisive to discuss the chemical enrichment of the ICM with yields and values of M/L consistently derived from the same IMF (see also the Appendix).

2.3.2. *The Abundance Ratios in the ICM*

We showed above that the Salpeter IMF can reproduce the observed iron enrichment if all the iron synthesized and not locked in the stars is shed into the ICM. We will now discuss the enrichment in α-elements.

Under the assumption that star formation in ellipticals is a fast process with a timescale $\lesssim$1 Gyr, as in standard GW models, the typical [O/Fe] ratio of stars formed over such timescales is $[{\rm O/Fe}] = +0.2$ (Table 1, col. [8], listing the typical [O/Fe] of the SSP ejecta up to an age $t = 1$ Gyr; see also Fig. 6*b*, *solid line*). This is in good agreement with the latest observational estimates of the α-enhancement in the bright elliptical galaxies that dominate the stellar mass in clusters (Trager et al. 2000a, 2000b; Mehlert et al. 2003). With a solar iron abundance in the stars (case A), $[{\rm O/Fe}] = +0.2$ corresponds to an oxygen abundance $X_{{\rm O},*} = 1.33 \times 10^{-2}$ (see footnote 2 above). With this value, from equations analogous

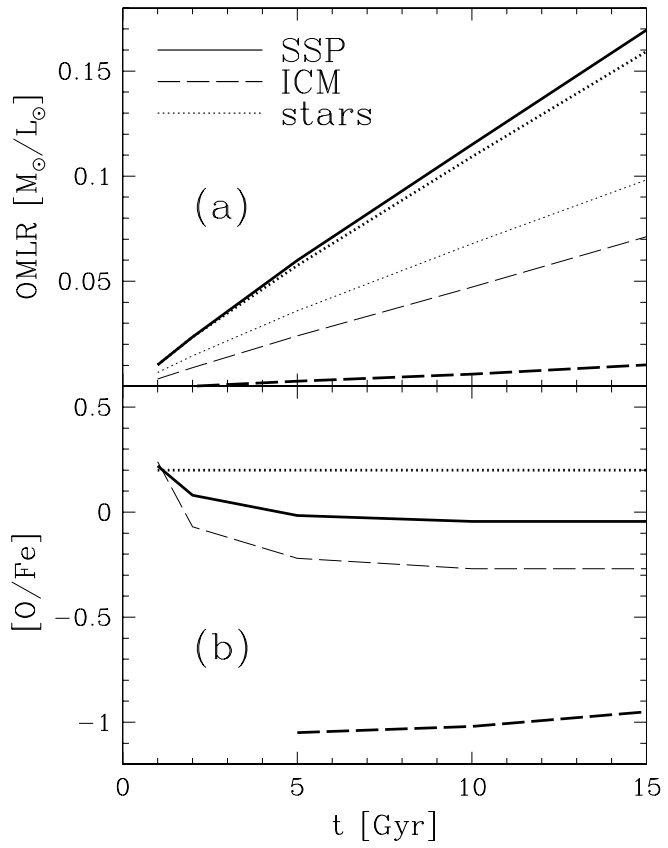

FIG. 6.—(*a*) Partition of the oxygen mass-to-light ratio between stars and ICM, for the Salpeter IMF; *thick lines*: case A for the stellar metallicities; *thin lines*: case B for the stellar metallicities (the "minimal" assumption; see text). Notice that while there can be equipartition of iron between stars and ICM (Fig. 5*a*), this is not the case for oxygen or α-elements: with the Salpeter IMF most of the oxygen produced is employed to build the observed stellar metallicities, and a very small fraction remains available to enrich the ICM. (*b*) Corresponding [O/Fe] ratio in the global ejecta, in the stars ([O/Fe] = +0.2 dex, assumed), and in the ICM; with the Salpeter IMF, the latter is strongly under solar even in case B (the most favorable to the ICM enrichment).

to equations (4) and (5) we calculate the oxygen mass MO_* locked in stars, and a negligible amount $MO_{\rm ICM}$ of the produced oxygen is left available to enrich the ICM (Table 3 and Fig. 6*a*, *thick lines*). So, if the late SN Ia products are released into the ICM and the observed $\rm IMLR_{ICM}$ is reproduced, this inevitably leads to strongly subsolar [α/Fe] ratios in the ICM (Figs. 6*b*, and 7*a* for the case of silicon). This was in fact the original prediction by Matteucci & Vettolani (1988), as well as the recent result by Pipino et al. (2002). However, such low abundance ratios are at odds with observations: low [α/Fe] ratios are observed only in the very central regions of clusters, probing the ISM abundances in the central cD galaxy rather than the ICM; the metallicity excess in "cool cores" (former cooling flows) is entirely due to the SNe Ia expected from the luminosity excess of the central bright galaxy and, in terms of mass, it represents only some 10% of the total metal mass in the ICM (De Grandi & Molendi 2001; De Grandi et al. 2003; Loewenstein 2004 and references therein). At large radii, where the bulk of the ICM mass resides, abundance ratios are *at least* solar (Finoguenov et al. 2000, 2003; Baumgartner et al. 2003; Renzini 2003 and references therein).

We may alternatively assume case B for the stellar metallicity, with solar values for the global metallicity and for ^{16}O and α-element abundances, and depressed iron abundance as following from the typical [O/Fe] = +0.2. In this case less metals are locked in the stars and the enrichment of the ICM is favored; the relevant stellar metallicities are $X_{\rm O,*} = X_{\rm O,\odot} = 8.3\times10^{-3}$ and $X_{\rm Fe,*} = 7.5\times10^{-4}$. With these values in equations (4) and (5), we obtain the partition in Table 4 and Figure 6 (*thin lines*). The conclusions remain largely unchanged: the observed $\rm IMLR_{ICM}$ can be reproduced only through late (after-GW) enrichment from SNe Ia; the consequent problem with the typical $\rm [O/Fe]_{ICM}$ is somewhat relieved, but the resulting $\rm [O/Fe]_{ICM} = -0.3$ is still quite low with respect to observations.

All in all, it seems very difficult to reproduce the observed $\rm IMLR_{ICM}$ with a Salpeter IMF, without violating constraints on the abundance ratios in the ICM. This is illustrated also in Figure 7*a* with the [Si/Fe] ratio (see § 2.4): at the old ages where the $\rm IMLR_{ICM}$ predicted with the Salpeter IMF reaches the observed levels (Fig. 7*c*), the corresponding [Si/Fe] is negative. Our computations confirm the well-known result that the Salpeter IMF predicts a "chemical asymmetry" with [α/Fe] > 0 in the stars and [α/Fe] < 0 in the ICM (Matteucci & Vettolani 1988; Renzini et al. 1993). That no such

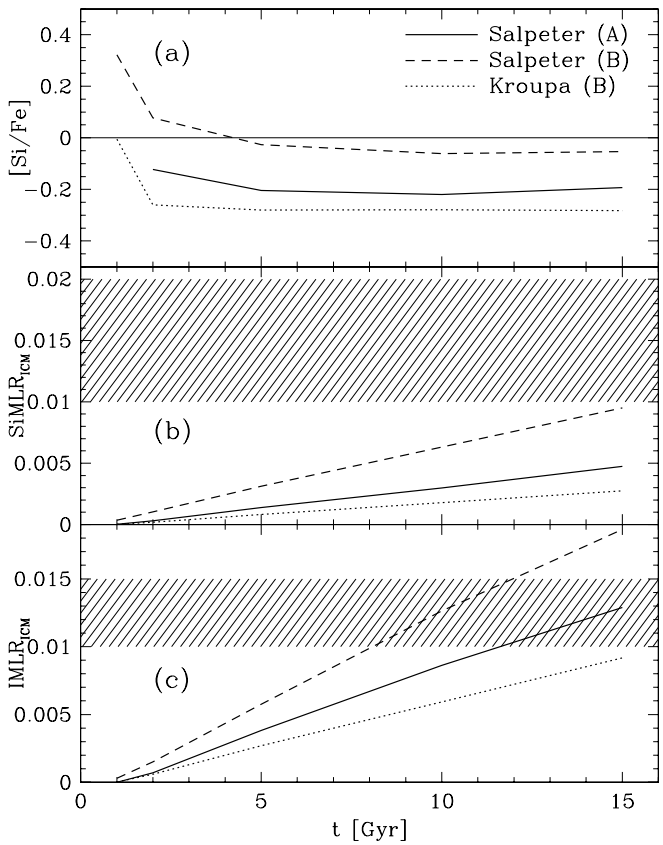

FIG. 7.—Predicted IMLR, SiMLR, and [Si/Fe] ratio in the ICM, as a function of the age of the stellar population; the shaded areas represent the observational range. All the metals not locked in the stars are assumed to be able to escape the galaxies and enrich the ICM. *Solid line*: Salpeter IMF with case A for the stellar metallicities; *dashed line*: Salpeter IMF with case B for the stellar metallicities (the "minimal" assumption, see text); *dotted line*: Kroupa IMF with case B. The Salpeter IMF can reach the observed level of IMLR at old ages (*c*); however, the predicted [α/Fe] ratios are then significantly under solar (*a*), at odds with observations. This reflects in the low predicted SiMLR, steadily below the observational level (*b*). With the "standard" Kroupa IMF, the predicted ICM enrichment is way below the observed levels at all times for both iron and silicon (*b*, *c*).

TABLE 4

PARTITION OF METALS BETWEEN STARS AND ICM WITH THE SALPETER IMF (CASE B)

t (Gyr) (1)	$M\mathrm{O}_*$ (2)	$M\mathrm{O}_{\mathrm{ICM}}$ (3)	$M\mathrm{Fe}_*$ (4)	$M\mathrm{Fe}_{\mathrm{ICM}}$ (5)	IMLR_* (6)	$\mathrm{IMLR}_{\mathrm{ICM}}$ (7)	$[\mathrm{O/Fe}]_{\mathrm{ICM}}$ (8)	$M\mathrm{Si}_*$ (9)	$M\mathrm{Si}_{\mathrm{ICM}}$ (10)	$\mathrm{SiMLR}_{\mathrm{ICM}}$ (11)
1.....	6.5E-3	3.5E-3	5.8E-4	2.9E-4	5.9E-4	2.9E-4	+0.24	5.4E-4	3.5E-4	3.5E-4
2.....	6.2E-3	3.8E-3	5.6E-4	6.4E-4	1.3E-3	1.5E-3	−0.07	5.2E-4	4.4E-4	1.0E-3
5.....	6.0E-3	4.0E-3	5.4E-4	9.6E-4	3.2E-3	5.7E-3	−0.22	5.0E-4	5.2E-4	3.0E-3
10.....	5.9E-3	4.1E-3	5.3E-4	1.1E-3	6.1E-3	1.3E-2	−0.27	4.9E-4	5.5E-4	6.3E-3
15.....	5.8E-3	4.2E-3	5.2E-4	1.1E-3	8.8E-3	1.9E-2	−0.27	4.8E-4	5.6E-4	9.5E-3

NOTES.—Col. (1): age of the SSP in gigayears; col. (2) oxygen mass locked in stars and remnants, assuming solar oxygen (and α-elements) abundance for $M_*(t)$ in Table 2; col. (3) remaining oxygen mass available to enrich the ICM; col. (4) iron mass locked in stars and remnants, assuming $[\mathrm{O/Fe}] = +0.2$; col. (5) remaining iron mass available to enrich the ICM; col. (6) IMLR of the stellar component, computed with the luminosity $L_B(t)$ in Table 2; col. (7) IMLR of the ICM, provided all the remaining iron can escape the galaxy; col. (8) [O/Fe] ratio in the ICM; col. (9) silicon mass locked in stars and remnants, assuming solar silicon (and α-elements) abundance for $M_*(t)$ in Table 2; col. (10) remaining silicon mass available to enrich the ICM; col. (11) SiMLR of the ICM, provided all the remaining silicon can escape the galaxy.

asymmetry is observed in real clusters is very difficult to explain within a standard chemical evolution scenario.

2.4. *The Silicon Mass-to-Light Ratio*

In the previous sections we discussed the predictions of the Salpeter IMF versus observations for the case of iron and oxygen. Iron is the element with the best-measured abundance in the ICM; oxygen is the main tracer of the global metallicity (roughly half of the global metals in the Sun), as well as of the α-elements, that is, of the typical products of SNe II. Observationally however, after iron the best-measured element in the ICM is silicon (Baumgartner et al. 2003), also an α-element mostly produced by SNe II—although the contribution of SNe Ia in this case is not negligible. The observed silicon mass-to-light ratio (SiMLR) in the hot ICM is $\mathrm{SiMLR}_{\mathrm{ICM}} = 0.01\text{–}0.02\ M_\odot/L_\odot$ (Finoguenov et al. 2000, 2003; Loewenstein 2004). In this section we compute and discuss the silicon production predicted from a Salpeter SSP.

With the chemical yields by Portinari et al. (1998), the silicon production from SNe II is somewhat metallicity dependent (with variations around 20%), but a representative average value from a Salpeter SSP of 1 $M_\odot$ is

$$M\mathrm{Si}_{\mathrm{II}} = 8 \times 10^{-4}\ M_\odot.$$

This corresponds to $[\mathrm{Si/Fe}] = +0.5$ as the typical abundance ratio due to SNe II (see the adopted solar abundances in footnote 2 above). This is compatible with the plateau level in halo stars (Cayrel et al. 2003), or even +0.1 dex high in Si production. Each SN Ia produces 0.154 $M_\odot$ of silicon (Iwamoto et al. 1999), so the SNe Ia in the SSP yield altogether

$$M\mathrm{Si}_{\mathrm{Ia}} = 2.5 \times 10^{-4}\ M_\odot$$

of silicon (Table 1), a smaller but nonnegligible contribution with respect to SNe II. In the last three columns of Table 1 we list the silicon production $M\mathrm{Si}_{\mathrm{Ia}}$ from SNe Ia, the total $M\mathrm{Si}_{\mathrm{tot}}$ from SNe Ia+SNe II, and the [Si/Fe] ratio of the cumulated ejecta as a function of time. In the last column of Table 2 we compute the corresponding $\mathrm{SiMLR}_{\mathrm{SSP}} = M\mathrm{Si}_{\mathrm{tot}}/L_B$. In the last three columns of Table 3 we compute the partition of silicon between stars and the ICM, with equations analogous to equations (4) and (5) and assuming case A for the stellar metallicities. The evolution of the global $\mathrm{SiMLR}_{\mathrm{SSP}}$ of a Salpeter SSP, as well as of the separate components $\mathrm{SiMLR}_{\mathrm{ICM}}$ and SiMLR_*, is plotted in Figure 5*b* (*thick lines*). From Figure 7*b* (*solid line*), the Salpeter SSP clearly falls short by at least a factor of 2 in explaining the observed SiMLR in the ICM. Even minimizing the amount of metals locked in the stellar component by assuming case B (Table 4), the predicted $\mathrm{SiMLR}_{\mathrm{ICM}}$ becomes at most marginally consistent with the lower limits of the observed range, and only for very large ages because of the very low luminosity (Fig. 7*b*, *dashed line*). However, with the presently favored cosmological scenario, Hubble constant value, and corresponding age of the universe, it seems unfeasible for the bulk of the stellar population in clusters to be as old as $\sim$15 Gyr.

The too-low resulting SiMLR is another signature that the Salpeter IMF does not produce enough α-elements to enrich the ICM to the observed levels.

2.5. *A Different Star Formation History?*

Our computations are based on a simple SSP approach that can be a reasonable approximation for an early and rapid star formation history. In this case we showed that if we require that the stars in elliptical galaxies have the observed solar metallicities and abundance ratios $[\alpha/\mathrm{Fe}] = +0.2$, it is difficult for the Salpeter IMF to reproduce the observed $\mathrm{IMLR}_{\mathrm{ICM}}$ without falling below solar $[\alpha/\mathrm{Fe}]$ ratios in the ICM (Figs. 6*b* and 7). One may wonder if agreement between the Salpeter IMF and observed abundance ratios in the ICM is possible once more complex star formation histories (SFH) are allowed for. In this section we argue against this possibility.

Suppose that we construct, with the Salpeter IMF, an ad hoc star formation history+wind/outflow history that produces a similar metal partition, and $[\alpha/\mathrm{Fe}]$ ratios, in the stars and in the ICM. This can only result in roughly solar ratios in both components, since the $[\alpha/\mathrm{Fe}]$ ratio of the global metal production is solar (Table 1 and Fig. 6*b*). Although it is doubtful that solar abundance ratios are representative of the bulk of stars in cluster ellipticals, we shall assume it for the sake of argument.

The required picture is likely to be a prolonged star formation history with a concurrent continuous partial outflow of metals. Stars keep forming, locking up a sizeable fraction of the delayed SN Ia products, while at the same time part of the metals keep escaping into the ICM. Such a prolonged SFH contrasts with the evidence that the bulk of the stellar population in ellipticals is old. But more important, the presence of a younger stellar component would substantially reduce the

TABLE 5
METAL PRODUCTION, LUMINOSITY, AND IMLR FROM A KROUPA SSP

t (Gyr) (1)	N_{Ia} (2)	$M\mathrm{Fe}_{tot}$ (3)	$M\mathrm{Si}_{tot}$ (4)	$\mathcal{M}_B$ (5)	L_B (6)	M_* (7)	M_*/L_B (8)	IMLR_{SSP} (9)	SiMLR_{SSP} (10)
1.....	4.7E-4	6.6E-4	5.9E-4	5.135	1.385	0.82	0.59	4.8E-4	4.3E-4
2.....	9.2E-4	9.7E-4	6.6E-4	5.969	0.643	0.79	1.22	1.5E-3	1.0E-3
5.....	1.4E-3	1.3E-3	7.3E-4	6.912	0.270	0.75	2.76	4.8E-3	2.7E-3
10.....	1.5E-3	1.4E-3	7.5E-4	7.589	0.145	0.72	4.98	9.6E-3	5.2E-3
15.....	1.6E-3	1.4E-3	7.6E-4	8.008	0.098	0.71	7.20	1.5E-2	7.8E-3

NOTES.—Col. (1:) age of the SSP in gigayears; col. (2) cumulative number of SNe Ia exploded up to age t; col. (3) total iron mass produced up to age t by SNe II+SNe Ia; col. (4) total silicon mass produced up to age t by SNe II+SNe Ia; col. (5) B-band magnitude of the SSP; col. (6) B-band luminosity of the SSP; col. (7) mass fraction of the initial 1 $M_\odot$ SSP remaining in stars and remnants; col. (8) M/L of the stellar (plus remnants) component of the SSP; col. (9) global IMLR of the SSP; col. (10) global SiMLR of the SSP.

global IMLR_{SSP} because of the increased luminosity (Table 3 and Fig. 1). We conclude that it would be unfeasible, with the Salpeter IMF, to reconcile a balanced distribution of metals and abundance ratios between stars and ICM while maintaining a high global IMLR_{SSP} at the same time.

3. PREDICTIONS WITH A "STANDARD" IMF

All the calculations in the previous section were performed for a Salpeter IMF with mass limits [0.1–100] $M_\odot$. This is often erroneously considered as a "standard" IMF (in the sense explained in § 1), but as anticipated in § 2 it is in fact *already too efficient* in metal enrichment, i.e., it has typical chemical yields (especially for oxygen and α-elements) too high to match the typical abundances in the solar neighborhood within the standard chemical evolution scenario (including infall and no outflows). With a Salpeter slope, an upper mass limit of 50–70 $M_\odot$, corresponding to a smaller number of SNe II and lower metal production, should rather be adopted to reproduce observations of the solar neighborhood and spiral galaxies in general (Tsujimoto et al. 1997; Thomas et al. 1998; Gratton et al. 2000; Portinari et al. 2004). The Scalo (1986) or Kroupa (1998) IMF, with a steeper slope at the high-mass end and lower yields, are better suited to model the local environment (Chiappini et al. 1997; Portinari et al. 1998; Boissier & Prantzos 1999).

The difference in (oxygen) yield between a Salpeter and a Kroupa IMF with the same mass limits [0.1–100] $M_\odot$ is a factor of ~1.7 (cf. Table 3 of Portinari et al. 2004). This difference is readily explained by considering equation (1): the shape of the IMF influences the net yield via the ratio $\zeta_9/(1-R)$, where ζ_9 is the amount of mass in stars with $M > 9\ M_\odot$, which become SNe II and produce the bulk of the metals; see Portinari et al. (2004) for a detailed discussion. The Salpeter and Kroupa IMFs have comparable locked-up fractions $1-R \sim 70\%$, but because of the steeper slope at the high-mass end, ζ_9 is about twice lower for Kroupa than for Salpeter (cf. Table 3 of Portinari et al. 2004). Henceforth, even if the Salpeter IMF were considered to be marginally consistent with the observed enrichment in clusters (disregarding the evidence from α-element abundances), the implied metal production is already twice higher than that of standard IMFs suited to reproduce the Milky Way.

From Figure 1 we can immediately see that the global iron production of a Kroupa SSP is also lower than that of a Salpeter SSP. At the same time, the typical luminosity of a Kroupa SSP is larger, because it has less mass locked in very low mass stars and an increased percentage of "intermediate-living stars" (around 1 $M_\odot$) with respect to the Salpeter IMF; the latter mass range is generally responsible for the bulk of the luminosity (Portinari et al. 2004). As a consequence of the lower iron yield and higher luminosity, the resulting Kroupa IMLR_{SSP} is substantially lower than for the Salpeter SSP. Therefore, we can anticipate that the Kroupa IMF will hardly be able to produce the observed IMLR in clusters of galaxies.

In this section we compute the expected chemical enrichment of the ICM from a really standard IMF (Kroupa 1998) with the same procedure we applied to the Salpeter IMF. Tables 5 and 6 are analogous to Tables 1 to 4 but for an SSP with the Kroupa IMF, and the results clearly show that with this really "standard" IMF one cannot explain the observed IMLR or SiMLR in clusters of galaxies (Fig. 7, *dotted line*). With the yields by Portinari et al. (1998), a 1 $M_\odot$ Kroupa SSP produces

$$M\mathrm{O}_{II} = 5.7 \times 10^{-3}\ M_\odot,$$

$$M\mathrm{Fe}_{II} = 3.3 \times 10^{-4}\ M_\odot,$$

$$M\mathrm{Si}_{II} = 5.2 \times 10^{-4}\ M_\odot$$

of ^{16}O, ^{56}Fe, and ^{28}Si from SNe II. In Table 5 we compute the rate of SNe Ia, the global metal production and the luminosity evolution for a Kroupa SSP. It is evident from Figure 1*d* and the tabulated $\mathrm{IMLR}_{SSP}(t)$ in Table 5 that the Kroupa IMF may match the observed $\mathrm{IMLR}_{ICM} \sim 0.015$ only for very high ages and provided *all* the iron produced is used to enrich the ICM with none left in the stellar component, which is unreasonable. The SiMLR_{SSP} is at all times lower than the levels greater than 0.01 observed in the ICM, which can never be matched (Fig. 5*d*).

In Table 6 we compute the partition of metals between stars and ICM. It is sufficient to consider only case B for the stellar metallicities (solar α-element abundances and $[\alpha/\mathrm{Fe}] = +0.2$) since this minimizes the metals locked in the stars and allows for a more efficient enrichment of the ICM. The resulting IMLR and SiMLR for the global SSP evolution and the partition between stars and ICM are plotted in Figures 5*c* and 5*d*.

Even with the most favorable case B assumption, the Kroupa IMF barely produces the oxygen mass needed to enrich the stars (Table 6, col. [2]), hence virtually no oxygen is left available to enrich the ICM. As anticipated above, the predicted IMLR_{ICM} becomes only marginally consistent with the observed one for extremely large ages, and then the corresponding $[\alpha/\mathrm{Fe}]$ ratio in the ICM is well subsolar, at odds with observations. The latter feature is reflected in the

TABLE 6

PARTITION OF METALS BETWEEN STARS AND ICM WITH THE KROUPA IMF (CASE B)

t (Gyr) (1)	$M\mathrm{O}_*$ (2)	$M\mathrm{Fe}_*$ (3)	$M\mathrm{Fe}_{\mathrm{ICM}}$ (4)	$\mathrm{IMLR}_{\mathrm{ICM}}$ (5)	$M\mathrm{Si}_*$ (6)	$M\mathrm{Si}_{\mathrm{ICM}}$ (7)	$\mathrm{SiMLR}_{\mathrm{ICM}}$ (8)	$[\mathrm{Si/Fe}]_{\mathrm{ICM}}$ (9)
1	6.8E-3	6.2E-4	4.4E-5	3.2E-5	5.7E-4	2.5E-5	1.8E-5	−0.01
2	6.5E-3	5.9E-4	3.8E-4	5.9E-4	5.4E-4	1.2E-4	1.8E-4	−0.27
5	6.2E-3	5.6E-4	7.3E-4	2.7E-3	5.1E-4	2.2E-4	8.0E-4	−0.29
10	6.0E-3	5.3E-4	8.6E-4	5.9E-3	5.0E-4	2.6E-4	1.8E-3	−0.28
15	5.9E-3	5.3E-4	9.0E-4	9.2E-3	4.9E-4	2.7E-4	2.8E-3	−0.28

NOTES.—Col. (1): age of the SSP in gigayears; col. (2) oxygen mass locked in stars and remnants, assuming solar oxygen (and α-elements) abundance for $M_*(t)$ in Table 5; col. (3) iron mass locked in stars and remnants, assuming $[\mathrm{O/Fe}] = +0.2$; col. (4) remaining iron mass available to enrich the ICM; col. (5) IMLR of the ICM, provided all the remaining iron can escape the galaxy; col. (6) silicon mass locked in stars and remnants, assuming solar silicon (and α-elements) abundance for $M_*(t)$ in Table 5; col. (7) remaining silicon mass available to enrich the ICM; col. (8) SiMLR of the ICM, provided all the remaining silicon can escape the galaxy; col. (9) [Si/Fe] ratio of the ICM.

very low $\mathrm{SiMLR}_{\mathrm{ICM}}$, lying below the observed one by a factor of 3 or more (Fig. 7, *dotted lines*).

4. DISCUSSION

In this paper we compute the metal production expected with a Salpeter IMF and the corresponding evolution of the global IMLR and SiMLR (Figs. 5*a* and 5*b*, *solid lines*). Then we compute the corresponding partition of metals and IMLR between stars and ICM (Figs. 5*a* and 5*b*, *dotted and dashed lines*).

We demonstrate that it may be possible to reproduce the observed IMLR in the ICM (Fig. 7*c*, *shaded area*) with a Salpeter IMF, provided all the metals ever produced and not locked in the stars are expelled from the galaxy and contribute to enriching the ICM, including the late SN Ia contribution. However, the SiMLR is not reproduced, and the predicted $[\alpha/\mathrm{Fe}]$ ratios are significantly under solar, as shown in Figure 7*a* and 7*b* (cf. the "chemical asymmetry"; Renzini et al. 1993). This is at odds with observations. These results obtained with a straightforward, simple computation qualitatively agree with results from more elaborated models following the detailed star formation and wind history of elliptical galaxies (Matteucci & Vettolani 1988; Pipino et al. 2002).

We remark also that the Salpeter IMF is *not* a "standard" IMF in the sense that it is not well suited to model the chemical evolution of the solar neighborhood; a Scalo or Kroupa IMF provides better predictions. On the other hand, with these IMFs it is impossible to account for the level of metal enrichment observed in clusters of galaxies, and not only for the α-elements but also for iron (Fig. 7, *dotted lines*). We also stress that it is not just the (possibly still uncertain) *abundance ratios*, but the *global* amount of metals observed in the ICM that points to a different IMF with respect to the solar neighborhood.

4.1. *Role of Uncertain Stellar Yields and Supernova Rates*

The results discussed above are robust with respect to uncertainties on (1) stellar and SN yields, and (2) the rate of SNe Ia.

1. One may argue that if theoretical nucleosynthesis calculations [the stellar yields $p_Z(M)$ in eq. (1)] are uncertain by an overall factor of $\sim$3, we may be grossly underestimating the metal production of any given IMF. Then, even a local (Scalo or Kroupa) IMF could produce the observed enrichment in galaxy clusters—which is a factor of 3 higher than that estimated in the solar neighborhood (eqs. [2] and [3] and Appendix).

Theoretical uncertainties in stellar yields of SNe II may be important to establish the *relative* contribution of SNe II and SNe Ia in the enrichment of the ICM (Gibson et al. 1997)—although the role of this uncertainty may be reduced, when one considers only those theoretical SN II yields that reproduce the observed tight $[\alpha/\mathrm{Fe}]$ plateau in halo stars (Cayrel et al. 2003). In terms of *global* metal production, however, the uncertainty in SN II yields seems to be below the required factor of 3 (see the Appendix), at least if we can estimate the real uncertainty in SN II models from comparing different sets of available SN yields.

More important, if stellar yields were a factor of 3 higher than adopted here, the same Scalo or Kroupa IMF could be hardly reconciled with the observed chemical evolution in the solar neighborhood. We underline in fact that the stellar yields adopted here do reproduce the solar neighborhood when combined with a Scalo/Kroupa IMF (Portinari et al. 1998) and that we scaled the most uncertain iron yield from SNe II so as to reproduce properly the observed $[\alpha/\mathrm{Fe}]$ plateau in halo stars (§§ 2.1 and 2.4). This makes our comparison between solar neighborhood and cluster enrichment as independent as possible of formal uncertainties in SN II yields, since we are using stellar yields that have been tested, and partly calibrated, to reproduce the solar neighborhood with the local Scalo/Kroupa IMF.

Besides, it is comforting that a number of different groups have modeled the solar neighborhood independently, each with their favorite set (or patchwork of sets) of stellar yields, and there is a general consensus that a Kroupa/Scalo IMF well reproduces the properties of the solar vicinity (Matteucci & François 1989; Chiappini et al. 1997; Portinari et al. 1998; Boissier & Prantzos 1999; Alibés et al. 2001; Liang et al. 2001; de Donder & Vanbeveren 2002; de Donder & Vanbeveren 2003), while a Salpeter IMF gives worse results both for the solar neighborhood (Tsujimoto et al. 1997; Thomas et al. 1998; Gratton et al. 2000) and for disk galaxies in general (Portinari et al. 2004). It seems that the gross overall picture for the solar neighborhood within standard chemical evolution models is well settled, in spite of the potential theoretical uncertainties in SN II yields.

If real stellar yields were significantly higher than the commonly adopted nucleosynthesis prescriptions in literature, to explain the solar neighborhood with such an excess of metal production one should invoke substantial metal losses from the disk—a nonstandard ingredient for chemical models of the Milky Way (see § 5).

2. Uncertainties about the progenitors of SNe Ia and in their evolution may well allow for SN Ia rates different from the

standard Greggio & Renzini (1983) formulation, adopted here and in most literature. With a different formulation, possibly the SN Ia rate in ellipticals was higher than predicted here, and/or more SN Ia ejecta could enrich the ICM to high levels of *iron*, even with a standard IMF. However, any attempt to compensate for the predicted low enrichment just by modifying the SN Ia rate, would not contribute significant α-elements and would decrease the [α/Fe] ratio in the ICM farther below solar values, at odds with observations. Therefore, adjusting the SN Ia contribution is not a viable solution to reconcile a standard IMF with the metal content in clusters.

4.2. *How is the IMF in Clusters?*

It is evident that the IMF in clusters of galaxies cannot be the Salpeter IMF—and even less so a standard solar neighborhood IMF. In this section we try to outline the qualitative features necessary for an IMF able to produce the observed chemical enrichment in clusters.

The net yield of a stellar population (eq. [1]) depends on the shape of the IMF essentially via the ratio $\zeta_9/(1-R)$, between the mass fraction ζ_9 "invested" in the progenitors of core-collapse supernovas that contribute the bulk of the metals ($M \geq 9\ M_\odot$), and the locked-up fraction $(1-R)$ (see Portinari et al. 2004, for a detailed discussion). The net yield can therefore be increased by increasing the number of massive stars and/or by reducing the locked-up fraction.

With respect to Salpeter, the cluster IMF should lock less mass in very low mass stars, with a correspondingly lower locked-up fraction and lower M/L. The latter feature would likely be in better agreement also with determinations of the dynamical M/L in ellipticals (Gerhard et al. 2001; Borriello et al. 2003). With such a "bottom-light" IMF the typical $\mathrm{IMLR_{SSP}}$, the relative numbers of SNe II and SNe Ia, and the corresponding global [α/Fe] ratio of the stellar ejecta, are not necessarily different from the Salpeter IMF. What changes is the global yield (eq. [1]) and the fraction of metals locked in stars, hence the partition of metals between the galaxies and the ICM is skewed in favor of the latter. In this case, within the early GW scenario enough metals may be dispersed into the ICM, reproducing the observed $\mathrm{IMLR_{ICM}}$ while preserving solar or moderately supersolar [α/Fe] both in the stars and in the ICM.

However, in clusters the global [α/Fe] ratio in the baryons seems to be somewhat supersolar—supersolar in the elliptical galaxies, at least solar in the ICM—therefore the relative SN II/SN Ia proportion is likely to be somewhat higher than that of the Salpeter IMF, which has typical solar ratios in the ejecta (§ 2.1). Somewhat shallower slopes than the Salpeter for $M > 1\ M_\odot$ are favored in this sense, although the quantitative details may depend on the assumed SN II yields (Gibson et al. 1997).

Definitely, the high-mass slope needs to be shallower than the Kroupa/Scalo one: the Kroupa IMF, in fact, in spite of being "bottom-light" with respect to Salpeter below $1\ M_\odot$, does not produce enough metals to explain clusters. Therefore, a larger ζ_9 (larger number of massive stars) is needed for the cluster IMF, than in the Kroupa IMF.

These qualitative features—high overall $\zeta_9/(1-R)$—are achieved, for instance, with the variable IMF scenario considered by Chiosi (2000) and Moretti et al. (2003), where the low-mass cutoff is skewed toward higher masses and the high-mass slope tends to be shallower at high redshifts and in larger galaxies; this scenario has also a number of advantages in explaining the spectrophotometric properties of ellipticals (Chiosi et al. 1998). Possibly, a similar result for the enrichment of the ICM can be obtained with an invariant IMF, provided it is characterized by a sufficiently high net yield (i.e., high $\zeta_9/1-R$) as described above.

5. CONCLUSIONS: TWO ALTERNATIVE SCENARIOS

From the previous discussion it is clear that a standard solar neighborhood IMF cannot explain the chemical enrichment of clusters of galaxies. We are then left with only two possible, alternative conclusions.

1. The IMF is different locally than in clusters. The variation probably depends on redshift as well as on local density and temperature conditions, as expected from theoretical arguments (Moretti et al. 2003 and references therein). Such a scenario could also explain the systematic differences between rich clusters and groups (Finoguenov et al. 2003) and the increasing level of α-element ICM enrichment with cluster temperature (Fukazawa et al. 1998, 2000; Finoguenov et al. 2000; Baumgartner et al. 2003).
2. The IMF is universal and invariant, but from cluster observations it must be far more efficient in metal production than we think and commonly assume in chemical models for the Milky Way. If this is the case, since we do not observe such high metallicities in disk galaxies, we must invoke substantial outflows of metals from spirals, too—and not only from the old bulge component resembling elliptical galaxies (Renzini 2002, 2003), but also throughout the disk evolution.

It seems the choice is between a nonstandard IMF or a nonstandard scenario for the chemical evolution of the solar neighborhood and disk galaxies. We will discuss the feasibility of either possibility in turn below.

5.1. *A Nonstandard IMF in Clusters*

As discussed in § 4.2, the key characteristic of the cluster IMF should be a low locked-up fraction, i.e., a smaller number of ever-lived, low-luminosity stars than in the Salpeter IMF, combined with a larger number of massive stars and SNe II than expected from the Scalo/Kroupa slope. We outline here some possible physical mechanisms to obtain a nonstandard IMF in clusters with these characteristics.

1. At high redshifts, the increasing temperature of the cosmic microwave background and the lower gas metallicity (i.e., reduced cooling efficiency) contribute to increase the temperature of the star-forming gas. Higher temperatures imply lower Mach numbers and less efficient turbulent compression, which is crucial to trigger the formation of low-mass stars. At increasing redshift, the Jean mass of the compressed gas clumps is expected to increase and the formation of low-mass stars is consequently hampered (Nordlund & Padoan 2003). In clusters, the bulk of star formation takes place at high redshift in elliptical galaxies, which favors a lack of low-mass stars with respect to solar neighborhood conditions.

A detailed discussion of the chemical evolution of the ICM within the scenario of a variable Jeans mass can be found in Moretti et al. (2003). A redshift dependence of the Jean mass could also explain the systematic differences between rich clusters and groups (Finoguenov et al. 2003). However, a more drastic variation than that expected from the sole cosmic background temperature seems to be required to reproduce the metal enrichment in clusters (Moretti et al. 2003; Finoguenov et al. 2003).

It is interesting that in starburst galaxies, with huge star formation rates resembling those that must have been typical

of the early elliptical galaxies, dynamical arguments favor low-mass cutoffs around 1–5 $M_\odot$, i.e., the absence of significant mass in low-mass stars (Leitherer 1998).

2. The mass of the largest star formed in a star cluster increases with total cluster mass, just as expected if stellar masses are drawn from a declining power-law probability distribution. The masses of star clusters follow themselves a mass function roughly $\propto M^{-2}$. The convolution of these two effects can explain the observed difference in the high-mass IMF slope between star clusters (Salpeter slope) and field (Scalo slope); see Kroupa & Weidner (2003); Kroupa (2003).

Large star clusters are more likely to form in large galaxies and/or in regimes of high star formation rate; in such a system, the net effect is to produce a larger number of massive stars, although the IMF distribution within each star cluster remains invariant (Kroupa & Weidner 2003). This effect can induce a more top-heavy *effective* IMF in ellipticals, where star formation is rapid and intense, with respect to disks, where the star formation history is smoother; hence an intrinsic difference is expected between clusters and disk galaxies like the Milky Way. Also, the IMF would be more top-heavy in massive galaxies with respect to smaller galaxies; this latter trend is the same as proposed, via a variable IMF, by Chiosi et al. (1998) to explain the ensemble of photometric properties of elliptical galaxies.

5.2. *A Universal IMF and Metal Outflows from the Disk*

If, alternatively, the IMF is universal and invariant, then to explain the observed metal enrichment in clusters its typical metal production (global yield) must be more efficient than usually assumed in the solar neighborhood, by a factor of 3 (eqs. [2] and [3] and Appendix).

In § 4.2 we argued for a "bottom-light" IMF in clusters (with respect to Salpeter). A bottom-light IMF is in fact also favored in the solar neighborhood from local star counts (Kroupa 2001, 2002; Chabrier 2003) and in disk galaxies in general, from arguments related to their low stellar M/L and the observed brightness of the Tully-Fisher relation (Portinari et al. 2004). The evidence that the IMF is everywhere bottom-light with respect to Salpeter below 1 $M_\odot$ also reduces, by about a factor of 2, the inferred star formation rate from the observed luminosities (Leitherer 1998; Cole et al. 2001).

The global yield of bottom-light IMFs tends to be high, because of the small amount of mass locked in low-mass stars (eq. [1]). At the same time, the IMF slope in the range of massive stars needs to be shallower than the Kroupa/Scalo slopes: these standard IMFs in fact, in spite of being bottom-light with respect to Salpeter, have been shown in this paper to be unable to produce enough metals to explain clusters. The IMF slope in the range of massive stars ($M > 10\ M_\odot$) determined in nearby young clusters and associations, as well as in starburst galaxies, is generally consistent with a Salpeter slope and therefore shallower than the Scalo one (Leitherer 1998; Massey 1998). Also, the observed cosmic rate of SNe II favors shallower slopes than the Scalo/Kroupa one for a universal IMF (Calura & Matteucci 2003).

Notice that shallower slopes than the Scalo one are compatible with observational determinations of the local IMF, since the high-mass slope is poorly determined and strongly depends on corrections for the binary fraction; slopes up to -1.3, about the Salpeter value, are possible (Kroupa 2001, 2002). Besides, global properties of spiral galaxies (notably, the Hα emission) seem to be better explained with shallower slopes than the Scalo one (Kennicutt et al. 1994; Sommer-Larsen 1996). It is in fact intriguing that some of the bottom-light IMFs considered by Portinari et al. (2004) to model the stellar M/L in disk galaxies do have yields comparable with the observed yield in clusters.

A higher global yield in the solar neighborhood can also be obtained maintaining a standard Kroupa/Scalo IMF, but invoking a significant (a factor of 3) underestimate in the stellar yields of massive stars; although we do not particularly favor this possibility (see § 4.1 and the Appendix).

Irrespective of the favored way (IMF or stellar yields) to obtain locally a global yield as high as in clusters, we do not observe that much metals in the solar neighborhood (cf. eqs. [2] and [3]) and a universal IMF that explains clusters necessarily requires substantial outflows of metals from galactic disks: at least 70% of the metals produced should be ejected (see the Appendix).

We foresee the following difficulties with this scenario. In disks, star formation proceeds at a smooth, non–burst-like pace, and although "fountains" and "chimneys" are observed, they do not have the necessary energy to escape the galactic potential (Bregman 1980; Dekel & Silk 1986; Heckman 2002); therefore winds are far less plausible in galactic disks than in spheroids. Although recent results indicate that winds are more common and ubiquitous than previously thought, even in our Galaxy and in normal star-forming galaxies (Veilleux 2003), what one observes is usually hot gas that escaped the disk; it is by no means obvious that this gas can escape into the intergalactic medium altogether and not just fall back onto the galaxy at some later time.

Moreover, from the dynamical point of view, strong ongoing stellar feedback and outflows could significantly hamper the progressive formation of galactic disks from the cool-out of halo gas (Sommer-Larsen et al. 2003; J. Sommer-Larsen, L. Portinari, & M. Laursen 2003 in preparation).

Finally, even though we may regard substantial metal outflows as a viable scenario, they certainly represent a "non-standard picture" for the chemical evolution of the solar neighborhood, which would demand a revision of our understanding of the formation and evolution of the disk of the Milky Way.

We benefitted from discussions with K. Pedersen, J. Andersen, Å. Nordlund, F. Calura, and M. Riello. L. P., acknowledges kind hospitality from the Astronomy Department in Padova and from the Observatories of Helsinki and Tuorla upon various visits. This study is financed by the Danmarks Grundforskningsfond (through the establishment of TAC) and by the Italian MIUR.

APPENDIX

OBSERVED EFFECTIVE YIELDS IN THE SOLAR NEIGHBORHOOD AND IN CLUSTERS

In this appendix we will better quantify the difference between the effective yields observed in clusters and in the solar neighborhood, respectively (see eqs. [2] and [3]). In the hypothesis that the effective yield in clusters is representative of a universal

IMF, this estimate will give us an idea of how much metals must have outflown from the solar neighborhood to the intergalactic medium to reconcile with the low metal content observed locally. We will discuss iron and α-elements separately.

A1. THE SOLAR NEIGHBORHOOD

The local surface mass density is about 50 $M_\odot$ pc^{-2}, with negligible dark matter contribution (Kuijken & Gilmore 1991; Flynn & Fuchs 1994; Sackett 1997). The local gas surface density is about 10 $M_\odot$ pc^{-2} (Dame 1993). Henceforth, locally $M_{\rm gas} = 20\%$–25% M_*.

The iron abundance distribution of local stars peaks between -0.2 and -0.1 dex (Wyse & Gilmore 1995; Rocha-Pinto & Maciel 1996; Hou et al. 1998; Jørgensen 2000; Flynn & Morell 1997; Kotoneva et al. 2002). Assuming -0.15 dex (or $Z_{\rm Fe,*} = 0.7\ Z_{\rm Fe,\odot}$) as a representative value for the stellar iron abundance, and assuming a solar abundance in the gas, the observed iron yield in the solar vicinity is

$$y_{\rm Fe,SV} \sim \frac{0.7 Z_{\rm Fe,\odot} M_* + Z_{\rm Fe,\odot}[(0.2\text{–}0.25)\ M_*]}{M_*} = (0.9\text{–}0.95) Z_{\rm Fe,\odot}. \quad \text{(A1)}$$

As to the α-elements, the bulk of local disk stars range between $[{\rm O/Fe}] = -0.1$ and +0.3 dex and between $[{\rm Si/Fe}] = 0$ and +0.2 dex (Edvardsson et al. 1993). We can take therefore $[\alpha/{\rm Fe}] = +0.1$ dex as a representative average value; also, for $[{\rm Fe/H}] = -0.15$ dex where the metallicity distribution peaks, $[\alpha/{\rm Fe}] \sim +0.1$ in the data by Edvardsson et al. (1993). This implies $[\alpha/{\rm H}] = -0.05$ dex, or $Z_{\alpha,^*} = 0.9 Z_{\alpha,\odot}$ as a typical value for disk stars. Assuming still solar abundances for the gas, the local effective yield in α-elements is

$$y_{\alpha,\rm SV} \sim \frac{0.9 Z_{\alpha,\odot} M_* + Z_{\alpha,\odot}[(0.2\text{–}0.25)\ M_*]}{M_*} = (1.1\text{–}1.15) Z_{\alpha,\odot}. \quad \text{(A2)}$$

Therefore, the observed effective yield in the solar vicinity is about solar (within 10%) both for iron and for α-elements.

Notice that locally the baryonic mass is dominated by the stellar mass and hence the effective yield is very close to the stellar metallicity, while the metals in the gaseous phase give a small contribution. Henceforth, the uncertainty in the gas metallicity and in the $M_{\rm gas}/M_*$ ratio does not affect much the local effective yield. The situation is very different in clusters, where the gas mass dominates and the estimated $M_{\rm gas}/M_*$ ratio is crucial to determine the effective yield.

A2. CLUSTERS OF GALAXIES

From their accurate *BeppoSAX* iron abundance profiles, deprojected and convolved with the gas density profiles, De Grandi et al. (2003) derive an average iron abundance by mass in the ICM $Z_{\rm Fe,ICM} = 0.34 Z_{\rm Fe,\odot}$ (0.23 $Z_{\rm Fe,\odot}$ in the old photospheric scale by Anders & Grevesse 1989). The typical iron abundance in the stellar populations in clusters is between $[{\rm Fe/H}] = -0.2$ and 0 dex, or $Z_{\rm Fe,*} = (0.6\text{–}1) Z_{\rm Fe,\odot}$ (cases B and A considered in this paper, respectively; see § 2.3).

The crucial and most uncertain quantity entering the estimate of the effective yield is the mass in the stars, since in clusters this can be estimated only indirectly from the observed luminosity—hence the importance of accounting self-consistently for the stellar M/L, as we underline in this paper. Moretti et al. (2003) noticed that different samples in literature agree very well on a typical value $M_{\rm ICM}/L_B = 30\ h^{-1/2} = 36\ M_\odot/L_\odot$, while the derived $M_{\rm ICM}/M_*$ can vary a lot after the assumed M/L. In Figure 8*a* and 8*b* we show, as a function of the stellar M/L, the corresponding $M_{\rm ICM}/M_*$ ratio and the effective iron yield, calculated as

$$y_{\rm Fe,cl} \sim \frac{[(0.6\text{–}1) Z_{\rm Fe,\odot}] M_* + 0.34 Z_{\rm Fe,\odot} M_{\rm ICM}}{M_*}. \quad \text{(A3)}$$

The values of stellar M/L in Figure 8 range between the typical value for a Salpeter SSP, which is 10 Gyr old (a minimal age to reach the observed IMLR; § 2) and the extensively quoted value 6.4 $h = 4.5\ M_\odot/L_\odot$ estimated by White et al. (1993). The Salpeter value should be considered as an upper limit to the M/L (and consequently a lower limit to the $M_{\rm ICM}/M_*$ ratio and to the effective yield in clusters) since, as we extensively argue in the paper, the IMF (universal or not) is "bottom-light" with respect to Salpeter both in clusters and in the solar neighborhood. The M/L corresponding to a 10 Gyr old Kroupa SSP is also indicated.

Comparing the effective iron yield in Figure 8*a* with the local one estimated in equation (A1) (i.e., about solar), it is evident that the observed yield in clusters is at the very least a factor of 2, more likely a factor of 3–4, higher. If the cluster value is interpreted as representative of a universal IMF—and not of a different IMF than the local one—this implies that 70% of the metals ever produced by the Milky Way disk must have escaped into the intergalactic medium, for the metal content in the solar neighborhood is 3–4 times lower than expected from the cluster yield.

We shall now discuss whether an effective yield that is so much higher can be reconciled in principle with a Kroupa/Scalo IMF, within present uncertainties in the stellar yields [the $p_Z(M)$ in eq. (1)]. In our approach, the most uncertain iron yield from SNe II has been essentially calibrated to reproduce the observed $[\alpha/{\rm Fe}]$ plateau in halo stars (§§ 2.1 and 2.4). Therefore, the relevant stellar yield uncertainty is in the oxygen and silicon yields. Oxygen is a well-understood element theoretically since it is produced in hydrostatic nuclear burning stages, and stellar yields from different authors agree within a factor of 2; the uncertainty mainly comes from the assumed mass loss, convection treatment, and $^{12}{\rm C}(\alpha,\gamma)^{16}{\rm O}$ reaction rate (Gibson et al. 1997; Prantzos 1998). The silicon production is in principle more uncertain, being related to explosive nucleosynthesis; however, from the analysis by Gibson et al. (1997) it seems that available SN II yields in literature are in remarkable agreement for ^{28}Si (within 20%).

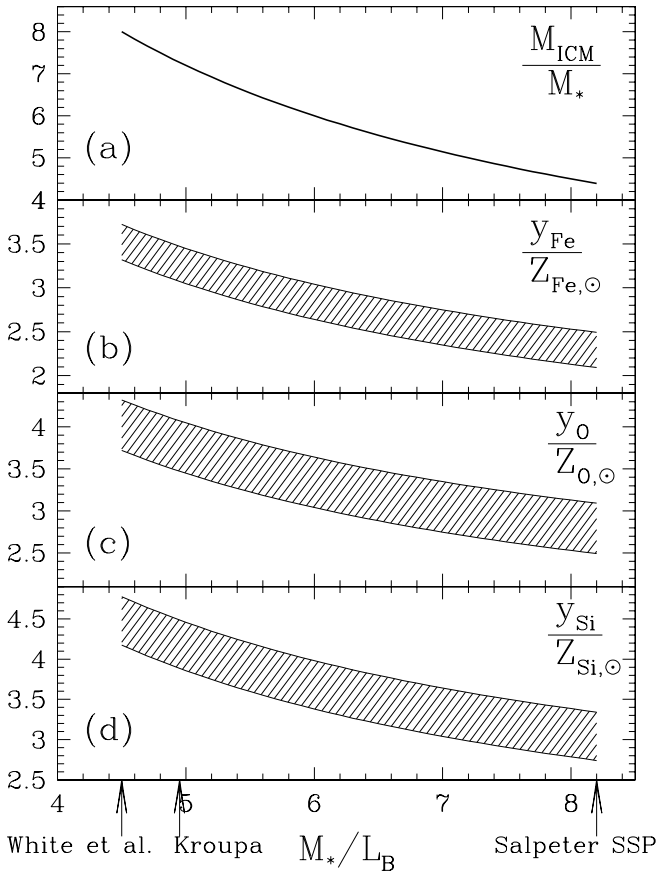

FIG. 8.—(*a*) ICM-to-star mass ratio, estimated from the observed $M_{\rm ICM}/L_B = 36\ M_\odot/L_\odot$ as a function of the assumed stellar M/L. (*b*) Corresponding iron effective yield, in solar units; the vertical range corresponds to different assumptions for the stellar metallicities (see text). (*c*) Corresponding oxygen effective yield, in solar units. (*d*) Corresponding silicon effective yield, in solar units.

From Figure 8 we see that for the stellar M/L expected from the Kroupa IMF, the iron yield in clusters is 3–3.5 times larger than solar (and for α-elements, the difference is up to a factor of 4–4.5; Figs. 8*c* and 8*d*). This is a much larger discrepancy than the factor of 2 expected from existing sets of SN II yields. Therefore, at least to the extent that different theoretical predictions in literature are a fair measure of the real uncertainties in stellar yields, it seems that the metal enrichment observed in clusters cannot be reconciled with the local Kroupa/Scalo IMF via the uncertainties in the SN II yields alone. We even argued in § 4.1 that, judging from the large number of independent models of the solar neighborhood adopting different sets of yields, the actual uncertainty in metal production related to the choice of stellar yields may be lower than that theoretically affecting the SN models. In fact, in our conclusions (§ 5) we favored either a variable IMF (different between clusters and disk galaxies) or a universal IMF that is different (in particular, shallower at the high-mass end) from the Kroupa/Scalo IMF.

The discrepancy in the observed effective yield between clusters and solar neighborhood is even more drastic when α-elements are considered, and it is α-elements, oxygen in particular, that define the bulk of the metal mass. Typical α-element abundances in the stellar populations in clusters are in the range $[\alpha/{\rm H}] = 0$ to +0.2 dex, or $Z_{\alpha,*} = (1\text{–}1.6)Z_{\alpha,\odot}$ (cases B and A in this paper, respectively). In the ICM $[\alpha/{\rm Fe}]$ abundance ratios are at least solar (e.g., the case of sulfur, Baumgartner et al. 2003), if not significantly supersolar (e.g., the case of silicon). For oxygen in particular, a solar abundance ratio $[{\rm O/Fe}] \sim 0$ seems to be appropriate if the updated solar iron abundance is adopted (Ishimaru & Arimoto 1997), which implies $Z_{\rm O,ICM} = 0.34Z_{\rm O,\odot}$ from the iron abundance determined by De Grandi et al. (2003) and adopted above in our calculations. We therefore compute the effective yield of oxygen in cluster as

$$y_{\rm O,cl} \sim \frac{\left[(1\text{–}1.6)Z_{\rm O,\odot}\right]M_* + 0.34Z_{\rm O,\odot}M_{\rm ICM}}{M_*} \tag{A4}$$

and plot it as a function of the assumed stellar M/L (i.e., $M_{\rm ICM}/M_*$ ratio) in Figure 8*c*. The oxygen yield in clusters is between 2.5 and 4 times larger than the local, solar one; a factor of 4 discrepancy corresponds to realistic bottom-light M/L.

Oxygen is, however, not particularly well measured in the ICM; silicon is the best-measured element after iron (Baumgartner et al. 2003). For this element, *ASCA* data provide SiMLR $\geq 0.01\ M_\odot/L_\odot$ (Finoguenov et al. 2000, 2003; Loewenstein 2004). For the stellar metallicity, we adopt $Z_{\rm Si,*} = (1\text{–}1.6)Z_{\rm Si,\odot}$, as for the α-elements in general (see above). Hence we can compute the effective silicon yield in clusters as

$$y_{\rm Si,cl} \sim \frac{\left[(1\text{–}1.6)Z_{\rm Si,\odot}\right]M_* + M_{\rm Si,ICM}}{M_*}, \tag{A5}$$

where

$$\frac{M_{\rm Si,ICM}}{M_*} = \frac{\rm SiMLR}{M_*/L_B} = \frac{0.01}{M_*/L_B},$$

and we plot the results in Figure 8*d*. The observed silicon yield in clusters is much larger, a factor of 3 to 4.5—with the latter being more realistic—than the local observed solar yield. And we have been conservative in our calculations, since we adopted the lower limit of the observational range SiMLR = 0.01–0.02 $M_\odot/L_\odot$ (Finoguenov et al. 2000, 2003). In fact, the silicon abundance and [Si/Fe] ratios in the ICM are so large that some contribution from exotic Population III hypernovas may be needed to produce it (Loewenstein 2001).

All in all, the effective yield in clusters is, with respect to the local solar one, about 3 times higher for iron and 4 or more times higher for α-elements. This difference is too large to be compensated by uncertainties in stellar nucleosynthesis alone, which are a factor of 2 or less. If this discrepancy is not the result of a cluster IMF different from the standard solar neighborhood one but is representative of some universal IMF acting both in clusters and in the Milky Way, then winds and outflows must have ejected into the intergalactic medium 70% of the metals actually produced in the solar neighborhood. A challenge indeed, for models of the evolution of disk galaxies.

REFERENCES

Alibés, A., Labay, J., & Canal, R. 2001, A&A, 370, 1103
Anders, E., & Grevesse, N. 1989, Geochim. Cosmochim. Acta, 53, 197
Arimoto, N., Matsushita, K., Ishimaru, Y., Ohashi, T., & Renzini, A. 1997, ApJ, 477, 128
Arnaud, M., Rothenflug, R., Boulade, O., Vigroux, L., & Vangioni-Flam, E. 1992, A&A, 254, 49
Balogh, M. L., Pearce, F. R., Bower, R. G., & Kay, S. T. 2001, MNRAS, 326, 1228
Baumgartner, W. H., Loewenstein, M., Horner, D. J., & Mushotzky, R. F. 2003, ApJ, submitted (astro-ph/0309166)
Boissier, S., & Prantzos, N. 1999, MNRAS, 307, 857
Borriello, A., Salucci, P., & Danese, L. 2003, MNRAS, 341, 1109
Bregman, J. N. 1980, ApJ, 236, 577
Calura, F., & Matteucci, F. 2003, ApJ, 596, 734
Cappellaro, E. 2001, Mem. Soc. Astron. Italiana, 72, 863
Cayrel, R., et al. 2003, A&A, in press (astro-ph/0311082)
Chabrier, G. 2003, PASP, 115, 763
Chiappini, C., Matteucci, F., & Gratton, R. 1997, ApJ, 477, 765
Chiosi, C. 2000, A&A, 364, 423
Chiosi, C., Bressan, A., Portinari, L., & Tantalo, R. 1998, A&A, 339, 355
Ciotti, L., D'Ercole, A., Pellegrini, S., & Renzini, A. 1991, ApJ, 376, 380
Cole, S., et al. 2001, MNRAS, 326, 255
Dame, T. M. 1993, in AIP Conf. Proc. 278, Back to the Galaxy, ed. S. S. Holt & F. Verter (Melville: AIP), 267
David, L. P., Forman, W., & Jones, C. 1991a, ApJ, 380, 39
———. 1991b, ApJ, 369, 121
de Donder, E., & Vanbeveren, D. 2002, NewA, 7, 55
———. 2003, NewA, 8, 415
De Grandi, S., Ettori, S., Longhetti, M., & Molendi, S. 2003, A&A, in press (astro-ph/0310828)
De Grandi, S., & Molendi, S. 2001, ApJ, 551, 153
Dekel, A., & Silk, J. 1986, ApJ, 303, 39
Edmunds, M. G. 1990, MNRAS, 246, 678
Edmunds, M. G., & Greenhow, R. M. 1995, MNRAS, 272, 241
Edvardsson, B., Andersen, J., Gustafsson, B., Lambert, D. L., Nissen, P. E., & Tomkin, J. 1993, A&A, 275, 101
Elbaz, D., Arnaud, M., & Vangioni-Flam, E. 1995, A&A, 303, 345
Finoguenov, A., Arnaud, M., & David, L. P. 2001, ApJ, 555, 191
Finoguenov, A., Burkert, A., & Böhringer, H. 2003, ApJ, 594, 136
Finoguenov, A., David, L. P., & Ponman, T. J. 2000, ApJ, 544, 188
Flynn, C., & Fuchs, B. 1994, MNRAS, 270, 471
Flynn, C., & Morell, O. 1997, MNRAS, 286, 617
Fukazawa, Y., Makishima, K., Tamura, T., Ezawa, H., Xu, H., Ikebe, Y., Kikuchi, K., & Ohashi, T. 1998, PASJ, 50, 187
Fukazawa, Y., Makishima, K., Tamura, T., Nakazawa, K., Ezawa, H., Ikebe, Y., Kikuchi, K., & Ohashi, T. 2000, MNRAS, 313, 21
Gal-Yam, A., Maoz, D., & Sharon, K. 2002, MNRAS, 332, 37
Gerhard, O., Kronawitter, A., Saglia, R. P., & Bender, R. 2001, AJ, 121, 1936
Gibson, B. K., Loewenstein, M., & Mushotzky, R. F. 1997, MNRAS, 290, 623
Gibson, B. K., & Matteucci, F. 1997a, MNRAS, 291, L8
———. 1997b, ApJ, 475, 47
Girardi, L., Bertelli, G., Bressan, A., Chiosi, C., Groenewegen, M. A. T., Marigo, P., Salasnich, B., & Weiss, A. 2002, A&A, 391, 195
Gratton, R. G., Carretta, E., Matteucci, F., & Sneden, C. 2000, A&A, 358, 671
Greggio, L., & Renzini, A. 1983, A&A, 118, 217
Grevesse, N., Noels, A., & Sauval, A. J. 1996, in ASP Conf. Ser. 99, Cosmic Abundances, ed. S. S. Holt & G. Sonneborn (San Francisco: ASP), 117
Grevesse, N., & Sauval, A. J. 1999, A&A, 347, 348
Heckman, T. M. 2002, in ASP Conf. Ser. 254, Extragalactic Gas at Low Redshift, ed. J. S. Mulchaey & J. Stocke (San Francisco: ASP), 292
Hou, J., Chang, R., & Fu, C. 1998, in ASP Conf. Ser. 138, 1997 Pacific Rim Conference on Stellar Astrophysics, ed. K. L. Chan, K. S. Cheng, & H. P. Singh (San Francisco: ASP), 143
Ishimaru, Y., & Arimoto, N. 1997, PASJ, 49, 1
Iwamoto, K., Brachwitz, F., Nomoto, K., Kishimoto, N., Umeda, H., Hix, W. R., & Thielemann, F. 1999, ApJS, 125, 439
Jørgensen, B. R. 2000, A&A, 363, 947
Jørgensen, I. 1999, MNRAS, 306, 607
Kennicutt, R. C. J., Tamblyn, P., & Congdon, C. E. 1994, ApJ, 435, 22
Kotoneva, E., Flynn, C., Chiappini, C., & Matteucci, F. 2002, MNRAS, 336, 879
Kroupa, P. 1998, in ASP Conf. Ser. 134, Brown Dwarfs and Extrasolar Planets, ed. R. Rebolo, E. L. Martin, & M. R. Zapatero Osorio (San Francisco: ASP), 483
———. 2001, MNRAS, 322, 231
———. 2002, Science, 295, 82
———. 2003, NewA Rev., 48, 47
Kroupa, P., & Weidner, C. 2003, ApJ, 598, 1076
Kuijken, K., & Gilmore, G. 1991, ApJ, 367, L9
Leitherer, C. 1998, in ASP Conf. Ser. 142, The Stellar Initial Mass Function, ed. G. Gilmore & D. Howell (San Francisco: ASP), 61
Liang, Y. C., Zhao, G., & Shi, J. R. 2001, A&A, 374, 936
Lin, Y.-T., Mohr, J. J., & Stanford, S. A. 2003, ApJ, 591, 749
Loewenstein, M. 2001, ApJ, 557, 573
———. 2004, in Origin and Evolution of the Elements, ed. A. McWilliam & M. Rauch (Cambridge: Cambridge Univ. Press), in press (astro-ph/0310557)
Loewenstein, M., & Mushotzky, R. F. 1996, ApJ, 466, 695
Maoz, D., & Gal-Yam, A. 2004, MNRAS, 347, 951
Marigo, P. 2001, A&A, 370, 194
Massey, P. 1998, in ASP Conf. Ser. 142, The Stellar Initial Mass Function, ed. G. Gilmore & D. Howell (San Francisco: ASP), 17
Matteucci, F., & François, P. 1989, MNRAS, 239, 885
Matteucci, F., & Gibson, B. K. 1995, A&A, 304, 11
Matteucci, F., & Vettolani, G. 1988, A&A, 202, 21
Mehlert, D., Thomas, D., Saglia, R. P., Bender, R., & Wegner, G. 2003, A&A, 407, 423
Moretti, A., Portinari, L., & Chiosi, C. 2003, A&A, 408, 431
Nordlund, Å., & Padoan, P. 2003, in Particle Physics in the New Millenium, ed. J. Tremtrempetiac & J. Wess (Lect. Notes Phys. 614; Berlin: Springer), 271
Pagel, B. E. J. 1997, Nucleosynthesis and Chemical Evolution of Galaxies (Cambridge: Cambridge Univ. Press)
———. 2002, in ASP Conf. Ser. 253, Chemical Evolution of Intracluster and Intergalactic Medium, ed. R. Fusco-Femiano & F. Matteucci (San Francisco: ASP), 489
Pipino, A., Matteucci, F., Borgani, S., & Biviano, A. 2002, NewA, 7, 227
Portinari, L., Chiosi, C., & Bressan, A. 1998, A&A, 334, 505
Portinari, L., Sommer-Larsen, J., & Tantalo, R. 2004, MNRAS, 347, 691
Prantzos, N. 1998, in ASP Conf. Ser. 147, Abundance Profiles: Diagnostic Tools for Galaxy History, ed. C. R. D. Friedli, M. Edmunds, & L. Drissen (San Francisco: ASP), 171

Renzini, A. 1997, ApJ, 488, 35
———. 2002, in ASP Conf. Ser. 253, Chemical Enrichment of Intracluster and Intergalactic Medium, ed. R. Fusco-Femiano & F. Matteucci (San Francisco: ASP), 331
———. 2003, in Clusters of Galaxies: Probes of Cosmological Structure and Galaxy Evolution, ed. J. S. Mulchaey, A. Dressler, & A. Oemler (Cambridge: Cambridge Univ. Press) (astro-ph/0307165)
Renzini, A., Ciotti, L., D'Ercole, A., & Pellegrini, S. 1993, ApJ, 419, 52
Rocha-Pinto, H. G., & Maciel, W. J. 1996, MNRAS, 279, 447
Sackett, P. D. 1997, ApJ, 483, 103
Salpeter, E. E. 1955, ApJ, 121, 161
Scalo, J. 1986, Fundam. Cosmic Phys., 11, 1
Sommer-Larsen, J. 1996, ApJ, 457, 118
Sommer-Larsen, J., Götz, M., & Portinari, L. 2003, ApJ, 596, 47
Tantalo, R., & Chiosi, C. 2002, A&A, 388, 396
Thomas, D. 1999, in Chemical Evolution from Zero to High Redshift, ed. J. R. Walsh & M. R. Rosa (Berlin: Springer), 197
Thomas, D., Greggio, L., & Bender, R. 1998, MNRAS, 296, 119
Tinsley, B. M. 1980, Fundam. Cosmic Phys., 5, 287
Tornatore, L., Borgani, S., Springel, V., Matteucci, F., Menci, N., & Murante, G. 2003, MNRAS, 342, 1025
Tozzi, P., Rosati, P., Ettori, S., Borgani, S., Mainieri, V., & Norman, C. 2003, ApJ, 593, 705
Trager, S. C., Faber, S. M., Worthey, G., & Gonzáles, J. J. 2000a, AJ, 119, 1645
———. 2000b, AJ, 120, 165
Trentham, N. 1998, MNRAS, 294, 193
Tsujimoto, T., Yoshii, Y., Nomoto, K., Matteucci, F., Thielemann, F.-K., & Hashimoto, M. 1997, ApJ, 483, 228
Veilleux, S. 2003, in in IAU Symp. 217, Recycling Intergalactic and Interstellar Matter ed. P. A. Due, J. Braine, & E. Brinks (San Francisco: ASP), in press
White, S. D. M., Navarro, J. F., Evrard, A. E., & Frenk, C. S. 1993, Nature, 366, 429
Woosley, S. E., & Weaver, T. A. 1995, ApJS, 101, 181
Wyse, R. F. G. 1997, ApJ, 490, L69
Wyse, R. F. G., & Gilmore, G. 1995, AJ, 110, 2771